Halo Nuclei in EFT

Renato Higa

Instituto de Física
Universidade de São Paulo

1st meeting of LIA - Subatomic Physics: from theory to applications

ITA, June 12-13, 2018

Outline

- motivation
- halo EFT: basic notions
- $\alpha\alpha$ scattering
- $n + {}^7\mathrm{Li} \to {}^8\mathrm{Li} + \gamma$
- ${}^3\mathrm{He} + \alpha \to {}^7\mathrm{Be} + \gamma$
- nd scattering
- Casimir-Polder forces
- Summary and outlook

NP opportunities

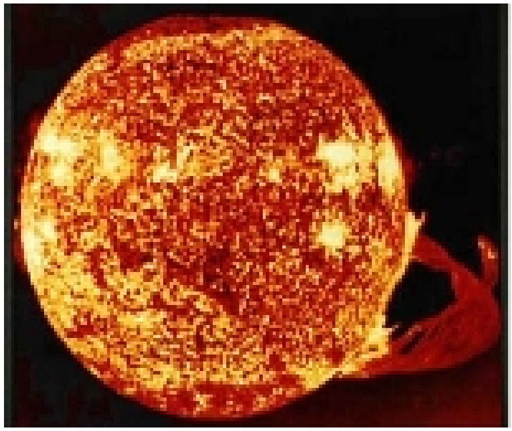

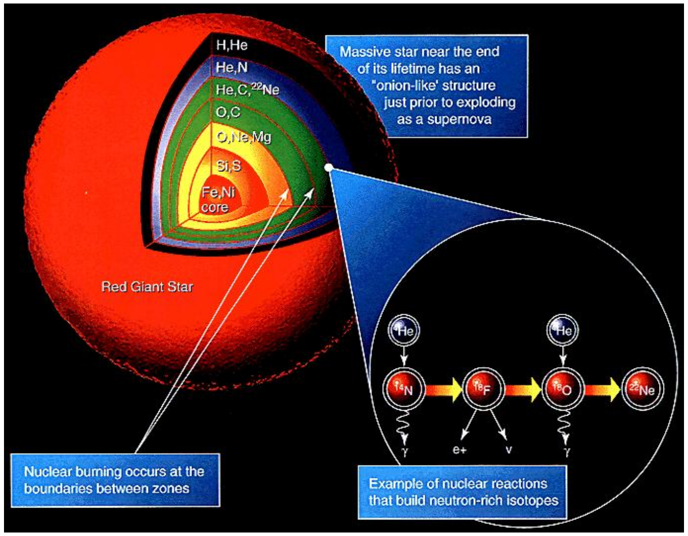

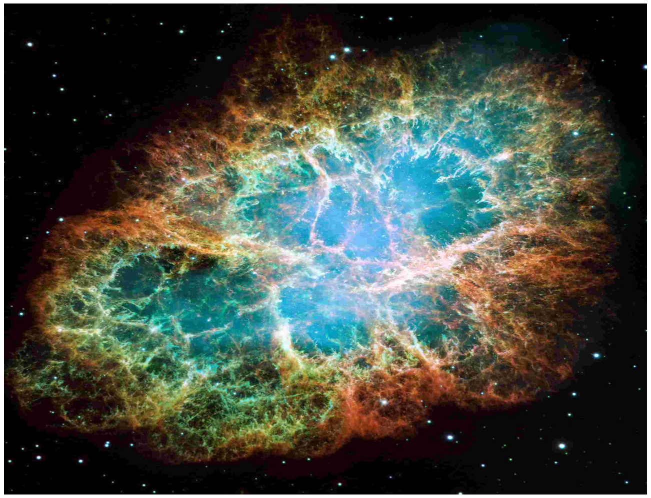

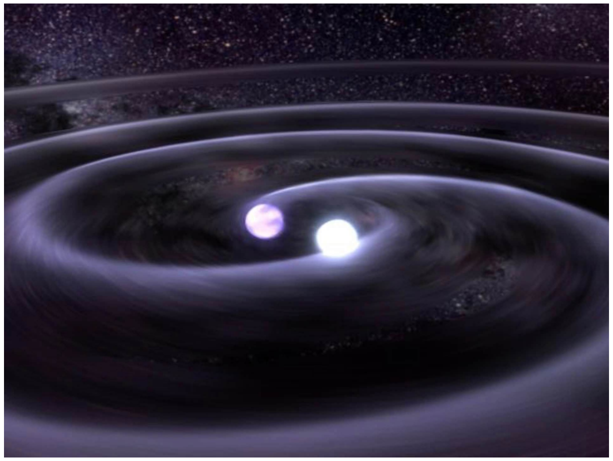

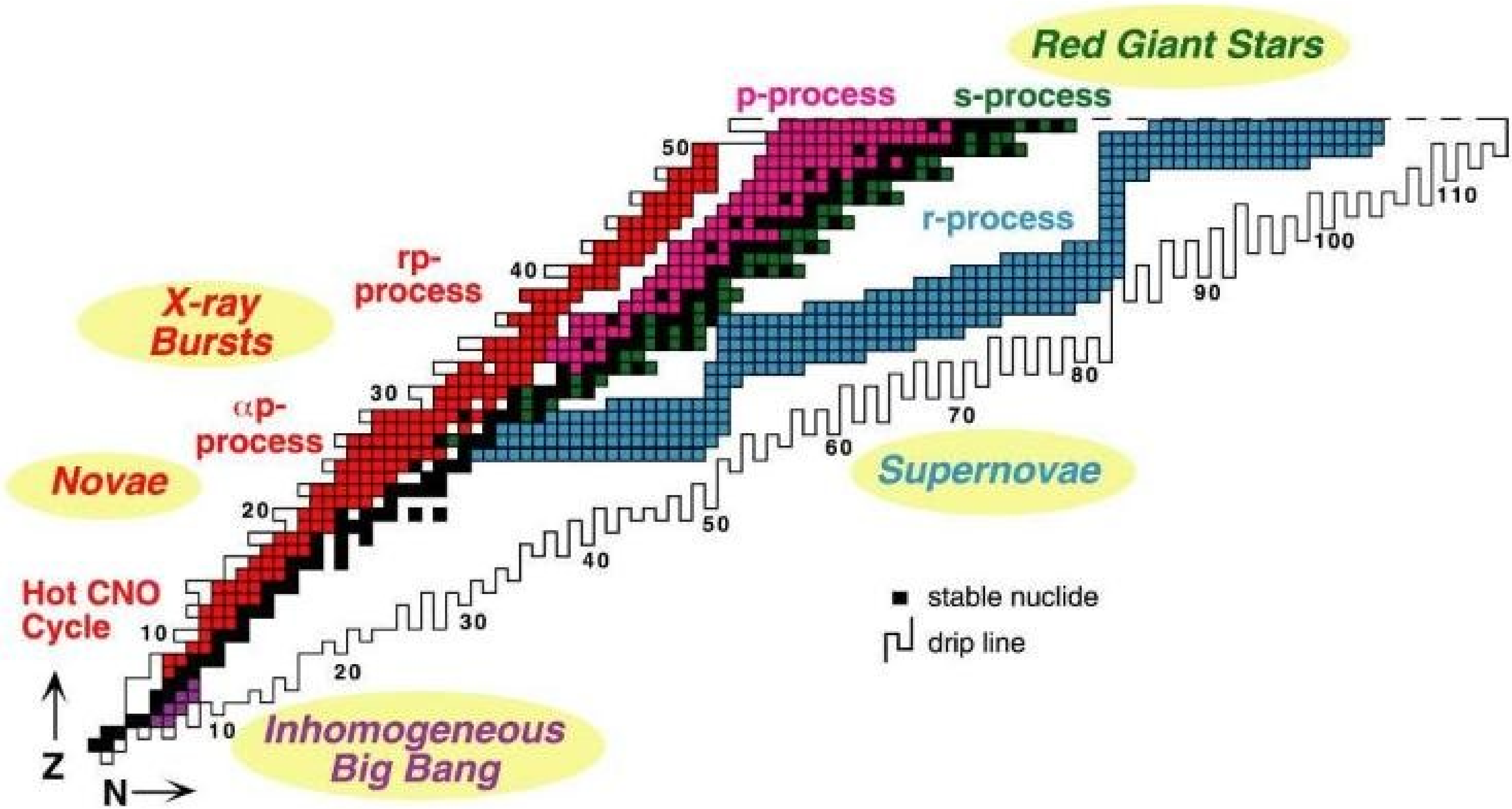
Red Giant Stars
p-process
s-process
r-process
rp-
process
X-ray
Bursts
αp-
process
Novae
Supernovae
Hot CNO
Cycle
Inhomogeneous
Big Bang
stable nuclide
drip line
Z
N

Effective Field Theories

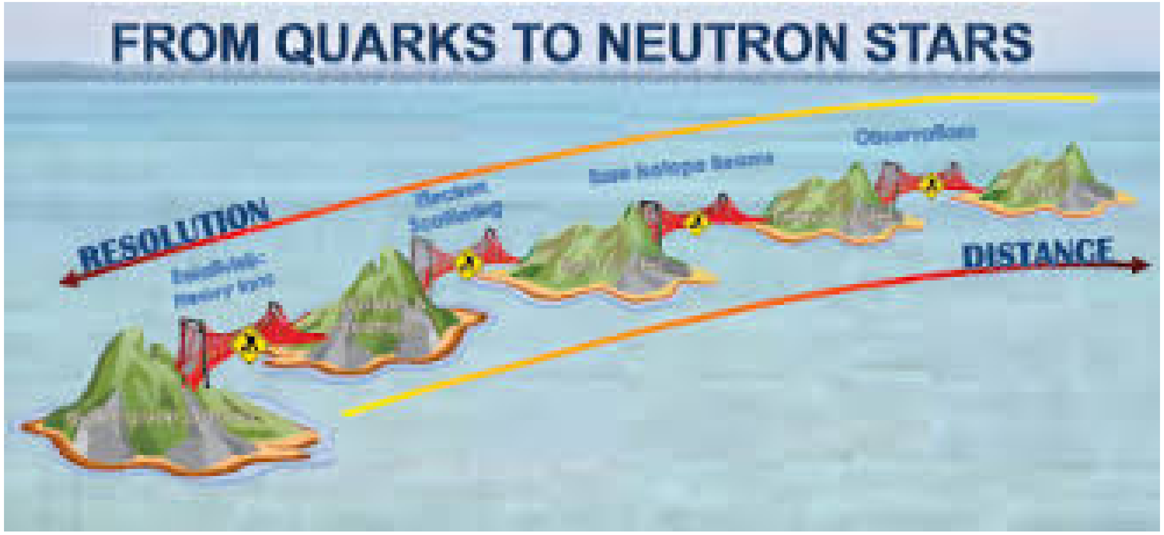

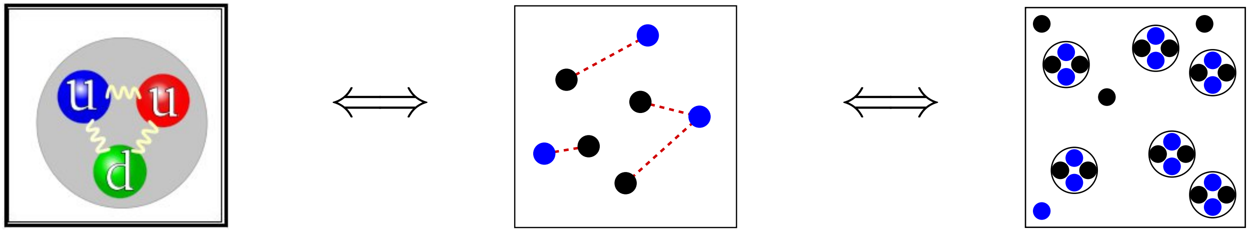

EFT: basic ideas

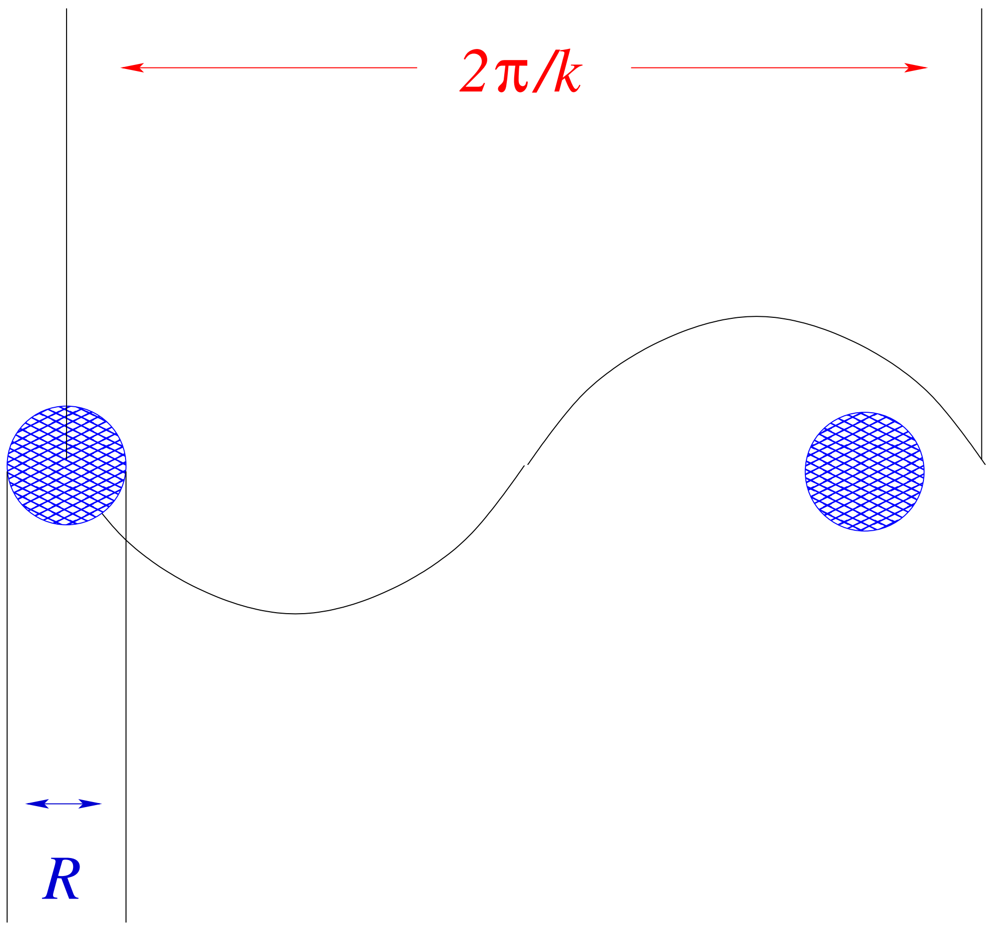

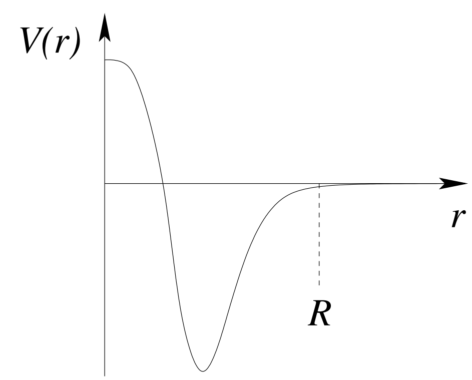

EFT: basic ideas

EFT with short-range interactions

$k \sim 1/a \sim M_{lo}\,, \quad 1/R \sim M_{hi}$

- 2-body: shallow bound state ($E_2 = \hbar^2/ma^2 + \cdots$), scaling limit @ LO
  RG flow towards a non-trivial fixed point (Birse *et al.*, ...)
  $|a| \to \infty$: unitary limit $\Rightarrow$ no scales (NR-conformal invariance)
- 3-body: correct renormalization requires a 3-body interaction at LO
  $\Rightarrow$ its functional dependence exhibits a limit cycle
- new paradigm in understanding the Thomas collapse and the Efimov effect

  Thomas: V_2 range $\to 0$, E_2 fixed
  $|E_3| \to \infty$

  Efimov: $|a| \to \infty$, large n
  $E_3^{(n+1)}/E_3^{(n)} \to e^{-2\pi/s_0}$
  $s_0 \approx 1.00624$

⋆ Efimov, Amado and Nobel, Adhikari *et al.*, Minlos and Fadeev, Frederico *et al.*, Fedorov *et al.*, ...

EFT and limit cycles: universality

(H.-W. Hammer and R.H., Eur. J. Phys. A 37, 193)

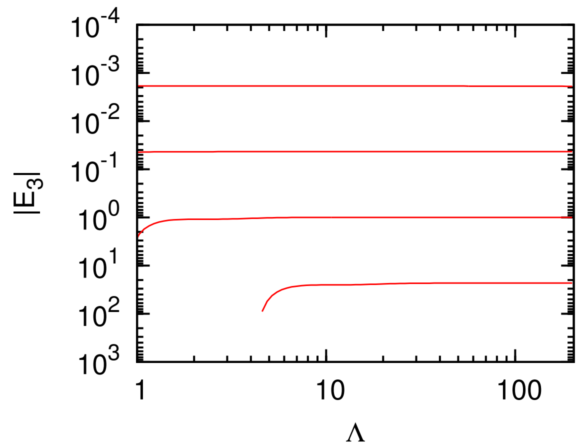

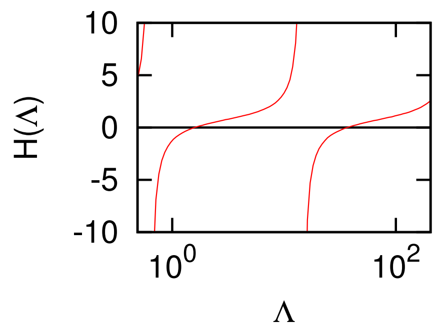

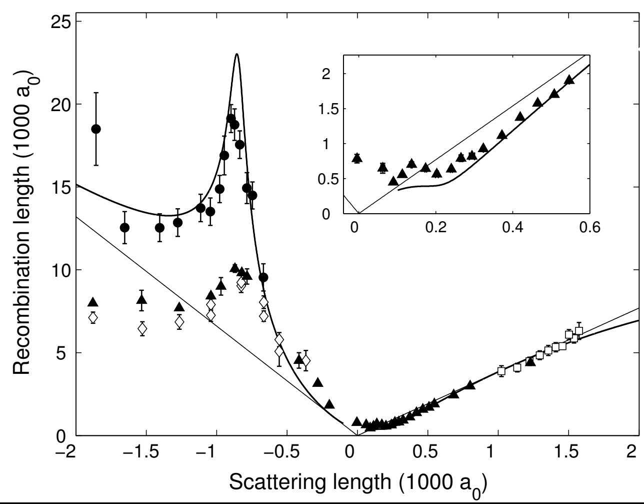

Recombination length in ultracold atoms

(T. Krämer *et al.*, Nature 440, 315; S. Knoop *et al.*, Nature Physics 5, 227; M. Zaccanti *et al.*, Nature Physics 5, 586; N. Gross *et al.*, PRL103, 163202)

- evidence for Efimov states
- universal functions provided by EFT

(E. Braaten and H.-W. Hammer, Phys. Rept. 428, 259)

pion mass dependence of a_{NN}

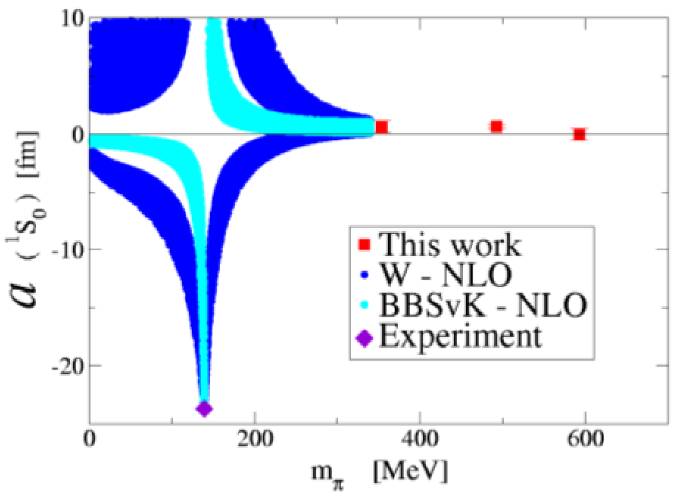

(NPLQCD: Beane *et al.*, PRL 97, 012001 (2006))

(see also Detmold *et al.*, PRL 116, 112301 (2016))

CHEN, LEE, LIU, AND LIU PHYSICAL REVIEW C 86, 054001 (2012)

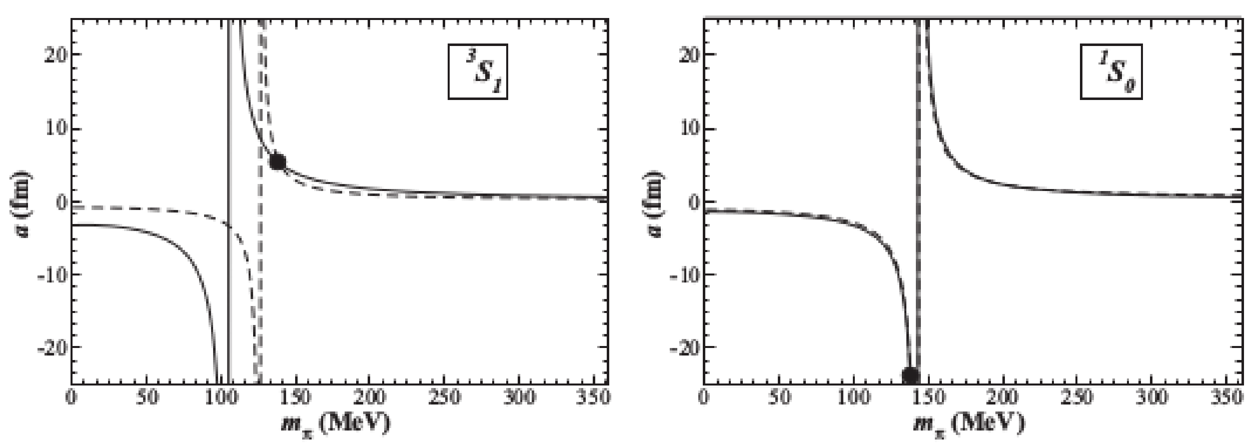

pion mass dependence of a_{NN}

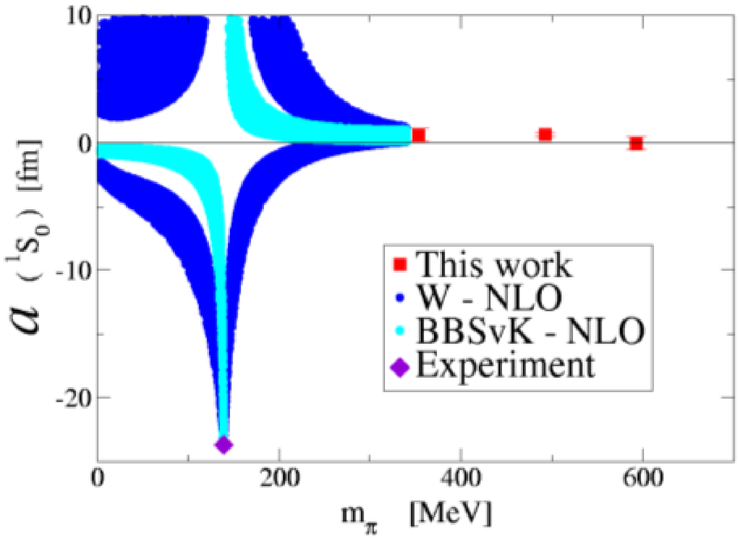

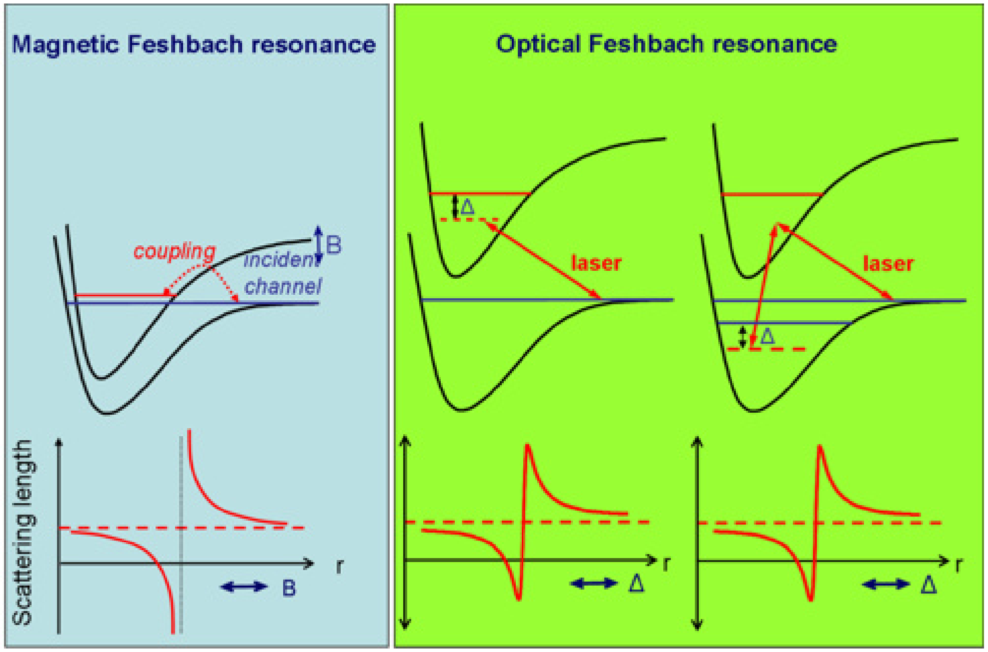

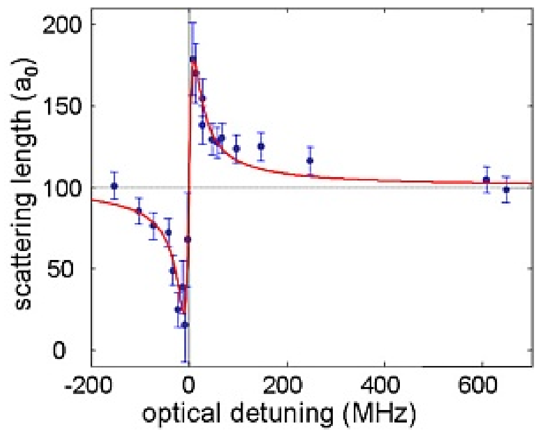

pion mass dependence of a_{NN}

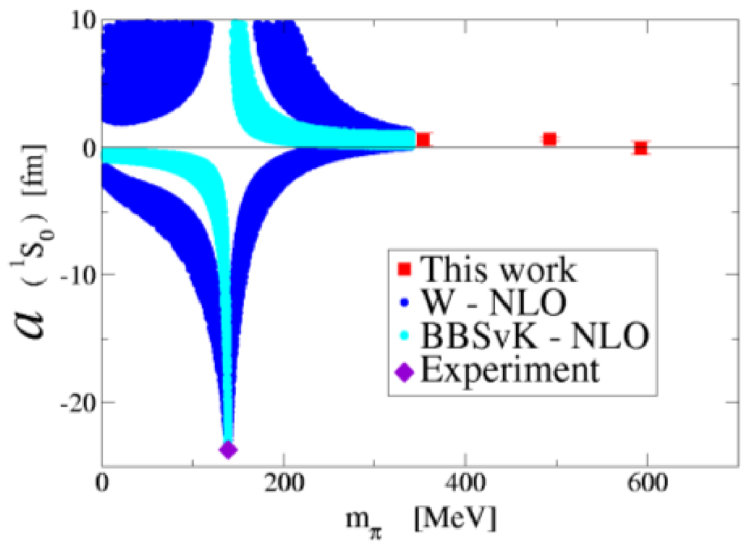

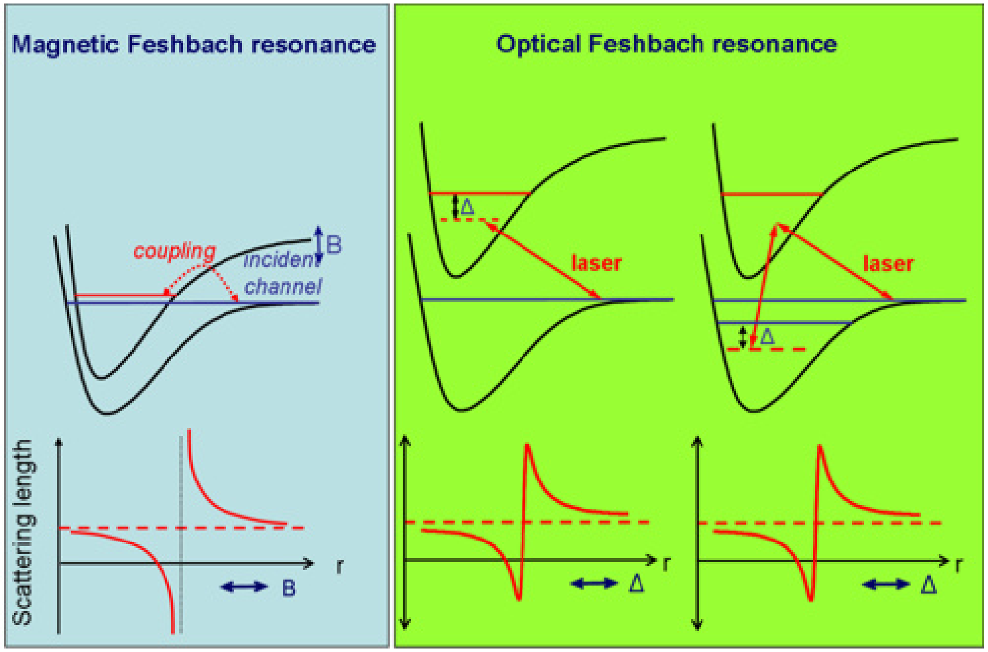

NP around the unitarity limit?

(König *et al.*, PRL118, 202501)

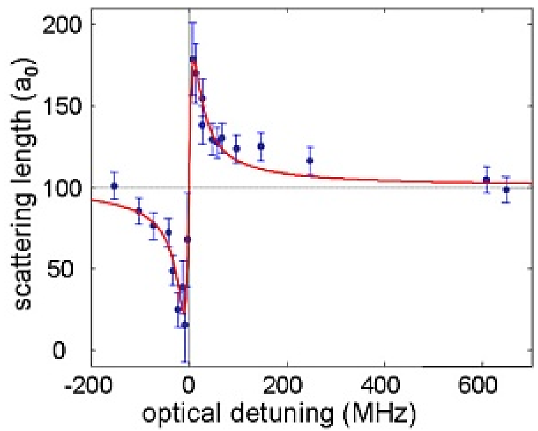

halo/cluster EFT: separation of scales

- excitation of each cluster $\sqrt{m_c E_c^*} \sim M_{hi}$ $(\gtrsim m_\pi)$
- binding of the valence nucleons (clusters) $\sim M_{lo} \ll M_{hi}$
- extension of the core—treated in *perturbation theory*
- power-counting: modified to account for other effects (resonance/Coulomb)
- expansion around the pole: rearrangement of the perturbative series, improved convergence
- Coulomb interactions

(Hammer, Ji, Phillips, J.Phys.G44, 103002)

potential models vs EFT

	V_{WS}	EFT
	$V_{WS}(r) = \frac{-V_0}{1+\exp\left(\frac{r-R}{d}\right)}$	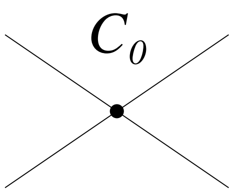
bound state	Sch. Eq. for V_0^B, SF/ANC	Feynman graphs, resum., $\mathcal{Z}$
scatt. states	Sch. Eq. for $V_0^{S,\nu}$	Feynman graphs (resum.), a, r
EM	$\mathcal{O}_{E1} = Z_C \frac{\mu}{M_C} e\, r\, Y_{1m}(\hat{r})$	QED

halo/cluster EFT: $k \ll m_\pi, \sqrt{m_c E_c^*} \sim M_{hi}$

Physical quantities: $k, 1/a_0 \sim M_{lo}$, $\quad r_0 \sim M_{hi}^{-1}, \mathcal{P} \sim M_{hi}^{-3}, \ldots$

$$T_l = -\frac{2\pi}{\mu} \frac{k^{2l}(2l+1)}{k^{2l+1}(\cot\delta_l - i)} P_l(\cos\theta)$$

$$k^{2l+1}\cot\delta_l \approx -1/a_l + \frac{r_l}{2}k^2 + \frac{\mathcal{P}_l}{4}k^4 + \cdots \qquad \text{(Bethe's ERE)}$$

$$\mathcal{L} = \phi^\dagger\left[i\partial_0 + \frac{\vec{\nabla}^2}{4\mu}\right]\phi + \sigma\, d^\dagger\left[i\partial_0 + \frac{\vec{\nabla}^2}{8\mu} - \Delta\right]d + g\left[d^\dagger\phi\phi + (\phi\phi)^\dagger d\right] + \cdots,$$

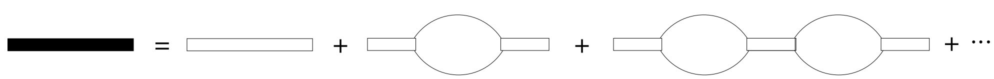

$$\Delta \sim M_{lo} \quad \rightarrow \quad iD_d^{(0)} = \frac{i\sigma}{-\Delta + i\epsilon} \sim \frac{1}{M_{lo}} \qquad (NN)$$

$$\Delta \sim M_{lo}^2/\mu \quad \rightarrow \quad iD_d^{(0)} = \frac{i\sigma}{q_0 - \boldsymbol{q}^2/8\mu - \Delta + i\epsilon} \sim \frac{\mu}{M_{lo}^2} \qquad (\alpha\alpha)$$

$\alpha\alpha$ scattering

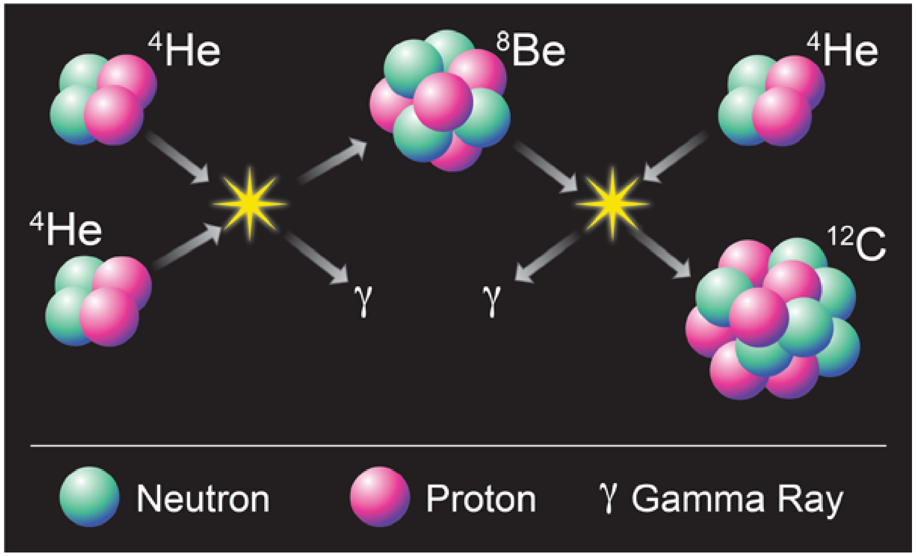

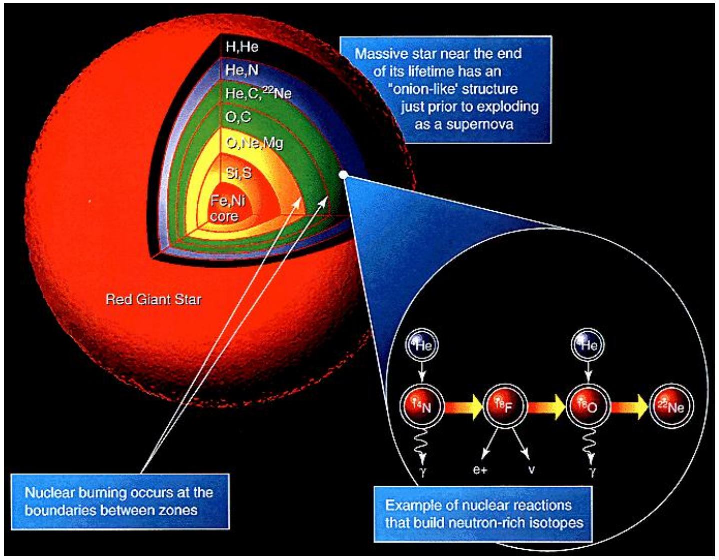

- input for the "reaction of life": $3\alpha \to {}^{12}\mathrm{C}$

(RH, Hammer, van Kolck, NPA 809, 171)

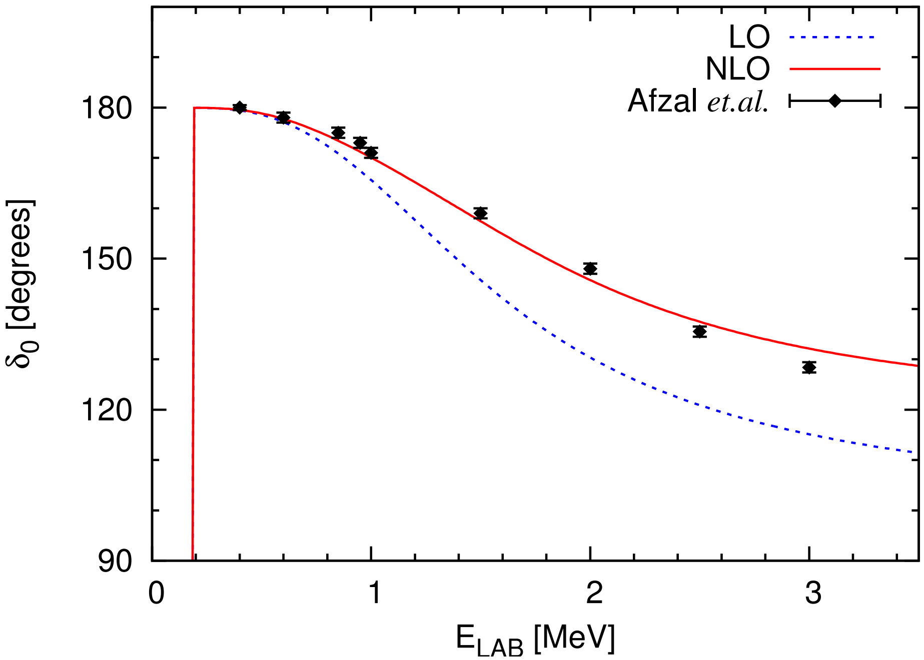

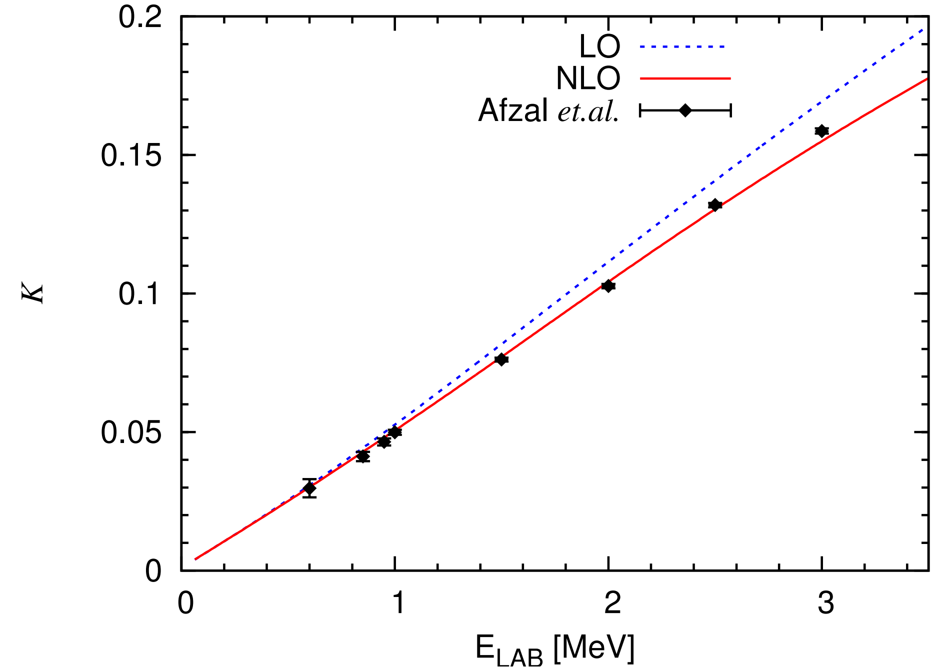

	a_0 (10^3 fm)	r_0 (fm)	$\mathcal{P}_0$ (fm^3)
LO	-1.80	1.083	—
NLO	-1.92 ± 0.09	1.098 ± 0.005	-1.46 ± 0.08
Rasche	-1.65 ± 0.17	1.084 ± 0.011	-1.76 ± 0.22

fine-tuning puzzle

$$\underbrace{\Delta^{(\mathrm{R})}}_{\frac{M_{hi}^2}{\mu}} = \underbrace{\Delta(\kappa)}_{\frac{M_{hi}^2}{\mu}} - \underbrace{\Delta^{(\mathrm{loops})}}_{\frac{M_{hi}^2}{\mu}} \qquad \text{(natural)}$$

$$\underbrace{\Delta^{(\mathrm{R})}}_{\frac{M_{hi}M_{lo}}{\mu}} = \underbrace{\Delta(\kappa)}_{\frac{M_{hi}^2}{\mu}} - \underbrace{\Delta^{(\mathrm{loops})}}_{\frac{M_{hi}^2}{\mu}} \qquad \text{(fine-tuned like } NN\text{)}$$

$$\underbrace{\Delta^{(\mathrm{R})}}_{\frac{M_{lo}^2}{\mu}} = \underbrace{\Delta(\kappa)}_{\frac{M_{hi}^2}{\mu}} - \underbrace{\Delta^{(\mathrm{loops})}}_{\frac{M_{hi}^2}{\mu}} \qquad \text{(fine-tuned to get } E_R\text{)}$$

$$\underbrace{\Delta^{(\mathrm{R})}}_{\frac{M_{lo}^3}{M_{hi}\mu}} = \underbrace{\Delta(\kappa)}_{\frac{M_{hi}^2}{\mu}} - \underbrace{\Delta^{(\mathrm{loops})}}_{\frac{M_{hi}^2}{\mu}} \qquad \text{(fine-tuned to get } \Gamma_R\text{)}$$

$\sim$ factor of 1000!!!

(Oberhummer *et al.*, Science 289, 88; RH, Hammer, van Kolck, NPA 809, 171)

^{7}Li$(n,\gamma)^8$Li

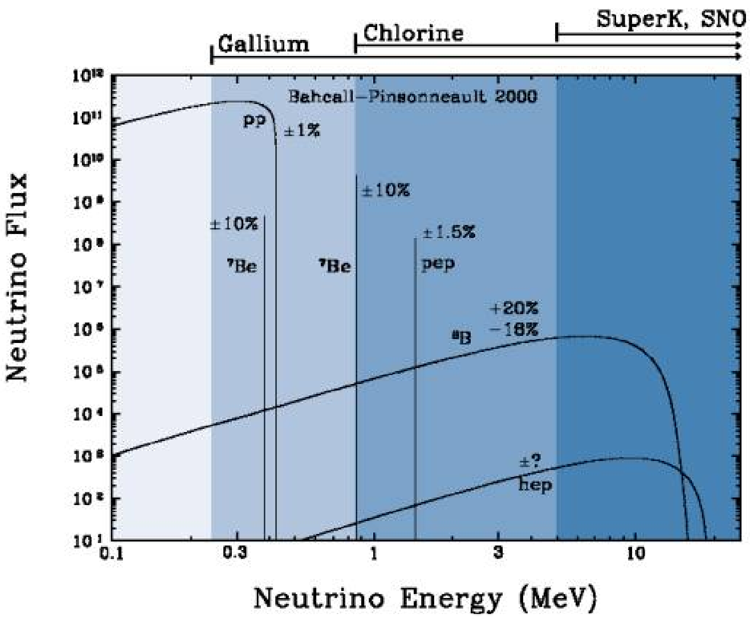

- $\mathrm{p} + {}^7\mathrm{Be} \rightarrow {}^8\mathrm{B} + \gamma$
  $\hookrightarrow {}^8\mathrm{Be} + e^+ + \nu_e$
  $\Rightarrow$ uncertainty on energetic ν_e flux
  $\Rightarrow$ $S_{17}(0)$: low-energy extrapolation
  $\Rightarrow$ matter/vacuum oscillations
  $\Rightarrow$ direct/inverse hierarchy

- mirror symmetry: ${}^7\mathrm{Li}(n,\gamma)^8\mathrm{Li}$
  - non-homogeneous BBN: bridge the A =8 gap
    ${}^1\mathrm{H}(n,\gamma)^2\mathrm{H}(n,\gamma)^3\mathrm{H}(d,n)^4\mathrm{He}(t,\gamma)^7\mathrm{Li}(n,\gamma)^8\mathrm{Li}$
    ${}^7\mathrm{Li}(n,\gamma)^8\mathrm{Li}(\alpha,n)^{11}\mathrm{B}(n,\gamma)^{12}\mathrm{B}(\beta^-)^{12}\mathrm{C}\ \ldots$

E_1 radiative capture

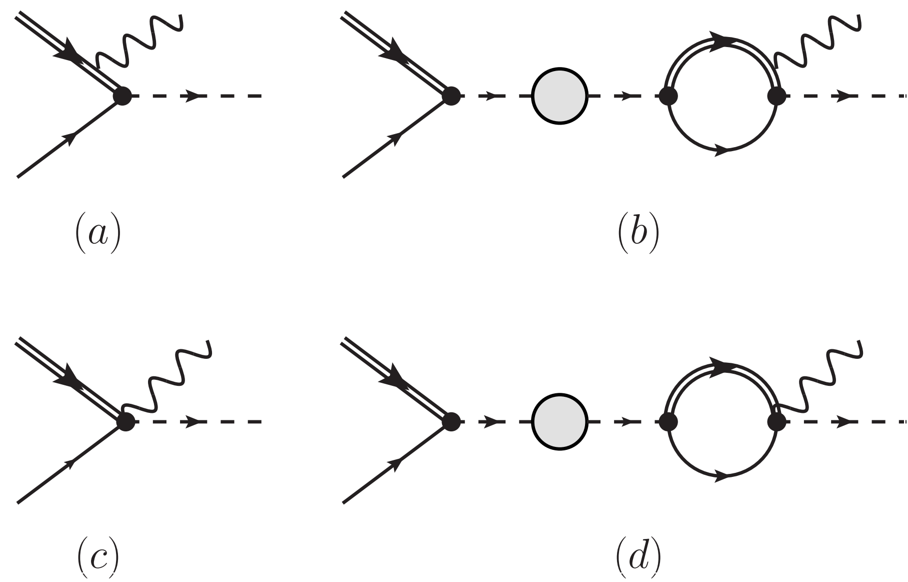

- gauge invariance: cancellation of divergences (Phillips and Hammer)

$$\sigma^{E_1}_{\rm capture} = \frac{\mathcal{Z}}{32\pi M^2}\frac{k_\gamma}{p}\,\alpha_{em}\left(\frac{Z_C M_N}{M}\right)^2 F(p,\gamma_B,M_C,M_N,a_0^{(1)},a_0^{(2)})$$

E_1 radiative capture

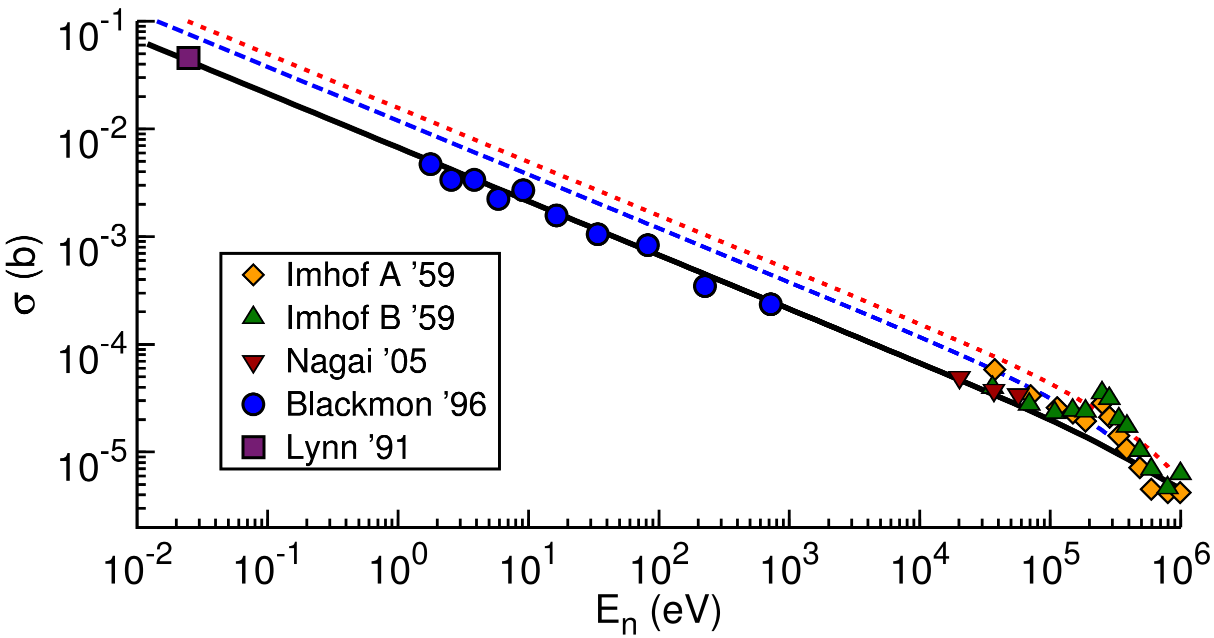

Davids-Typel: $r_1 \approx -0.30$ fm^{-1}

Tombrello: $r_1 \approx -0.46$ fm^{-1}

Wigner bound: $r_1 \lesssim -1$ fm^{-1}

E_1 radiative capture

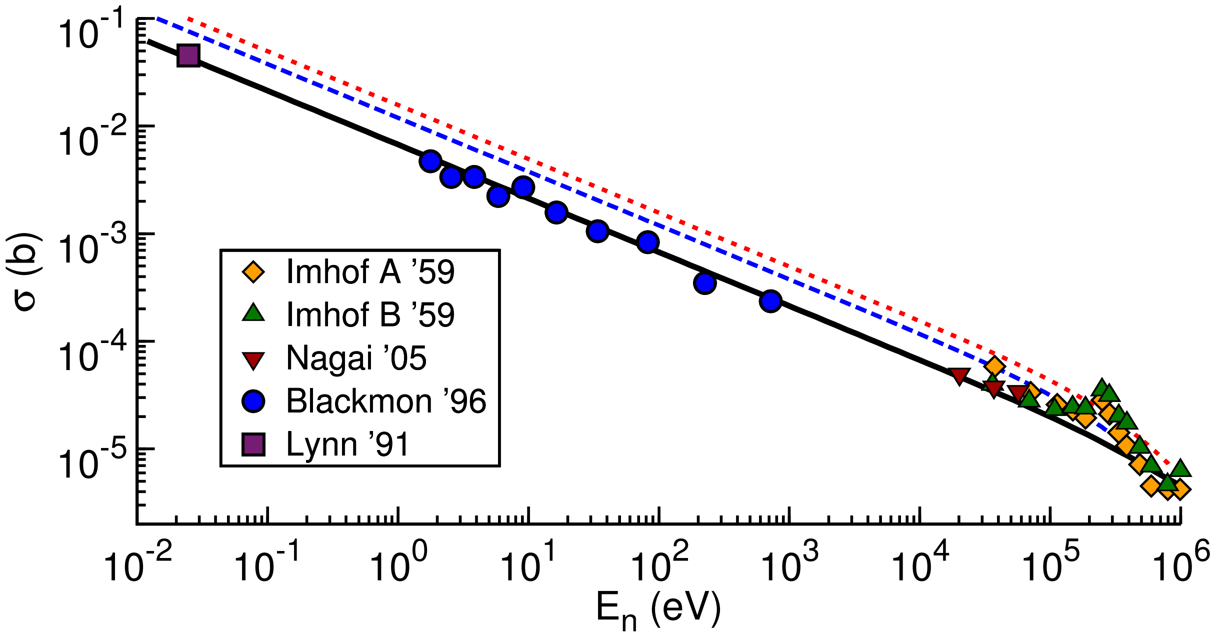

Davids-Typel: $r_1 \approx -0.30$ fm^{-1}

Tombrello: $r_1 \approx -0.46$ fm^{-1}

EFT: $r_1 = -1.47$ fm^{-1}

(G. Rupak, RH, PRL 106, 222501, 2011; L. Fernando, RH, G. Rupak, EPJA 48, 24, 2012)

E_1 radiative capture

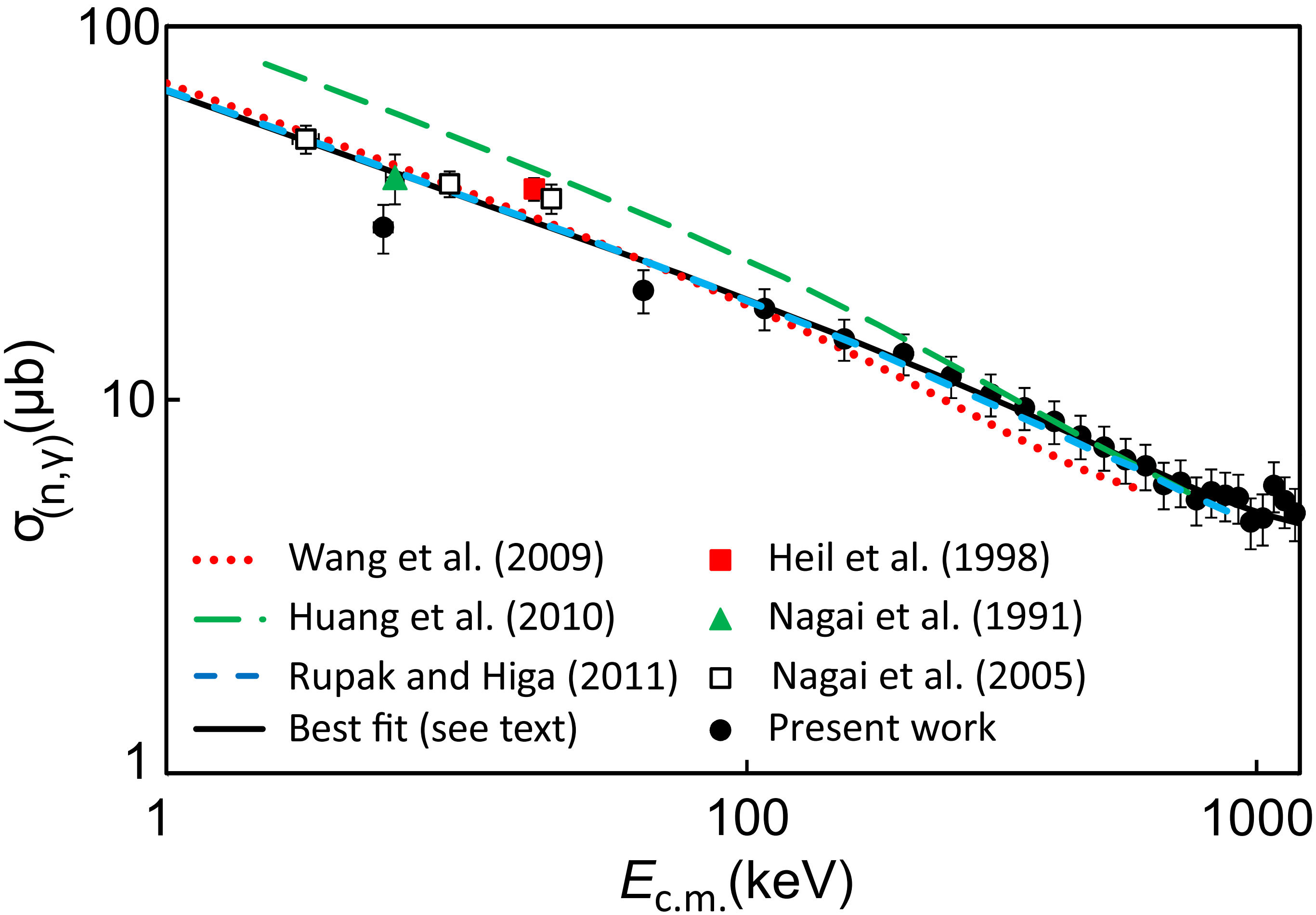

(Izsák *et al.*, PRC 88, 065808, 2013)

^{3}He$(\alpha,\gamma)^{7}$Be

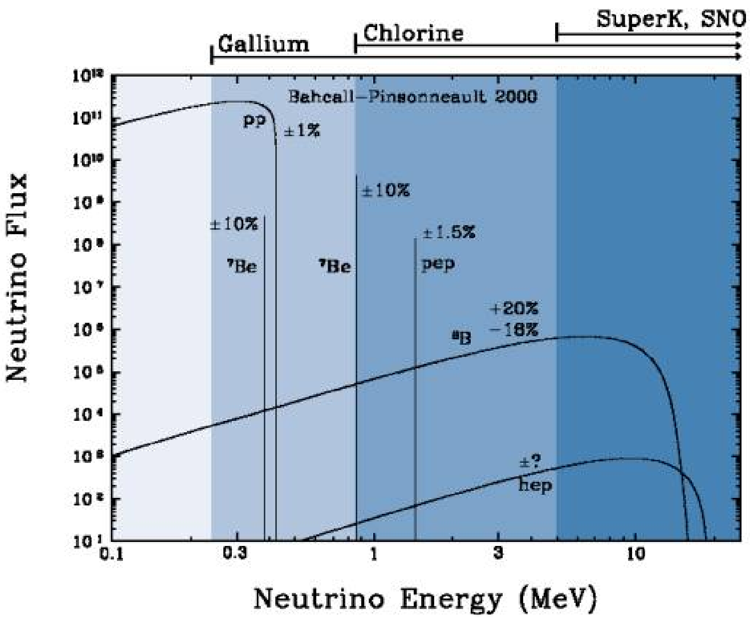

- $^{3}\mathrm{He} + \alpha \to {}^{7}\mathrm{Be} + \gamma$

  $\hookrightarrow {}^{7}\mathrm{Li} + e^{+} + \nu_e$

  $\Rightarrow$ uncertainty on mid-energy ν_e

  $\Rightarrow$ $S_{34}(0)$: low-energy extrapolation

  $\Rightarrow$ matter/vacuum oscillations

  $\Rightarrow$ direct/inverse hierarchy

- Lithium abundance in the universe

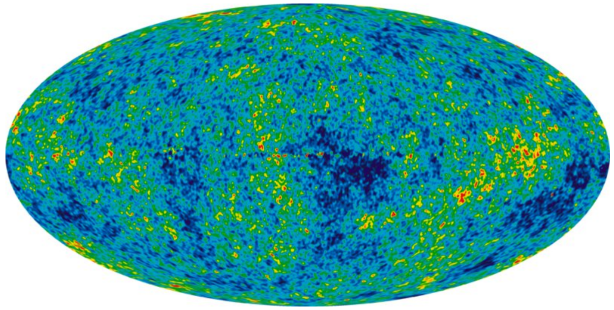

$^3\mathrm{He}(\alpha,\gamma)^7\mathrm{Be}$ radiative capture

- $^7\mathrm{Be}$: predominant $^3\mathrm{He}$-α cluster
- $B_0\,(^2P_{3/2}) \sim 1.6$ MeV, $B_1\,(^2P_{1/2}) \sim 1.2$ MeV $\ll S_p$ (~ 5.5 MeV), $E_\alpha^\star$ (~ 20 MeV)

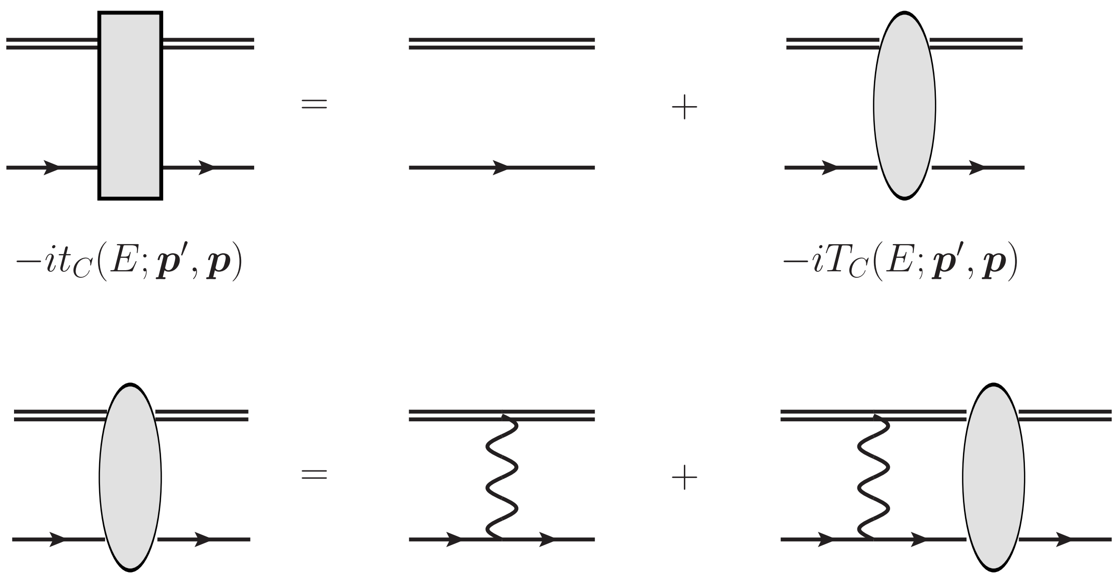

$^{3}\mathrm{He}(\alpha,\gamma)^{7}\mathrm{Be}$ radiative capture

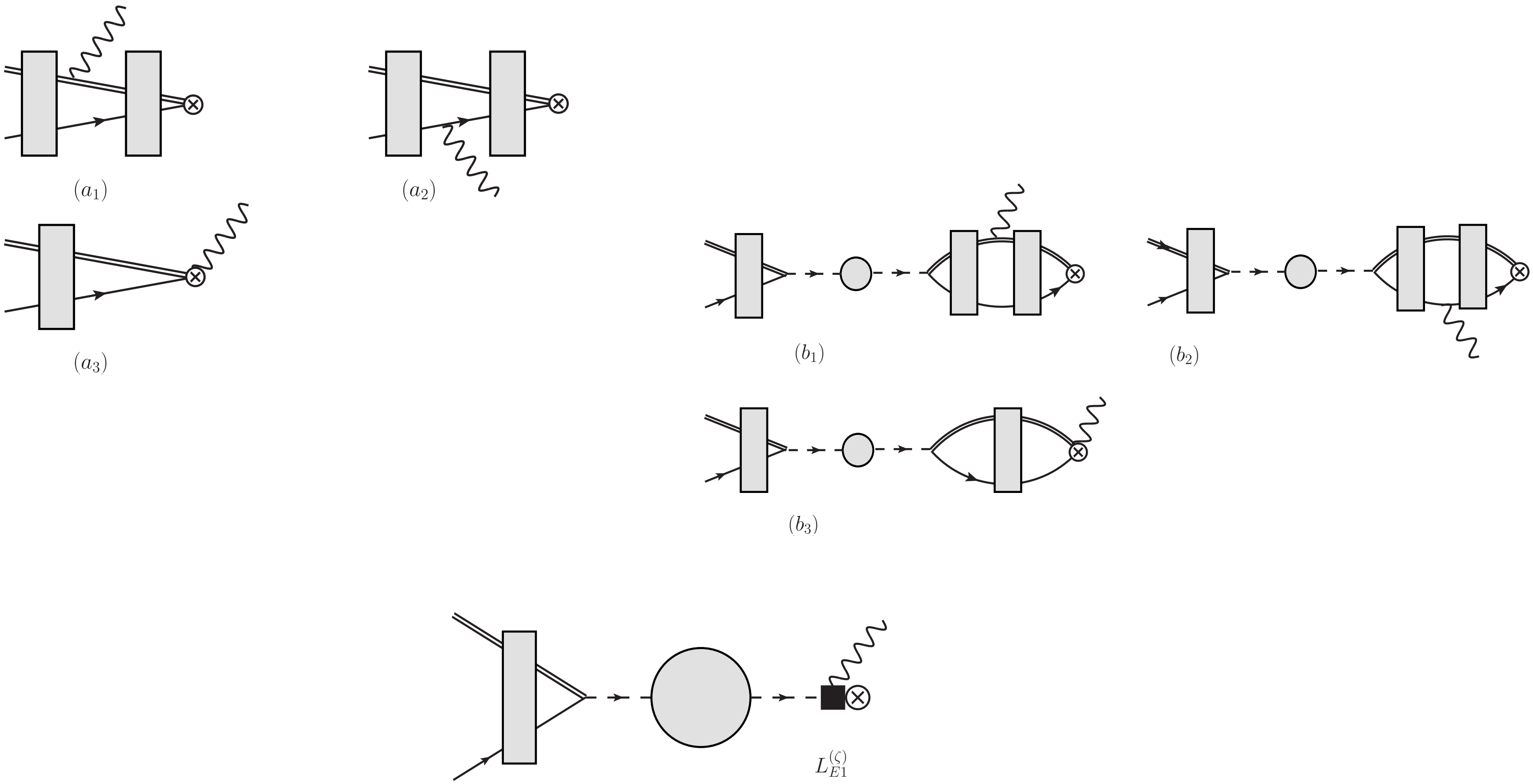

$^3\mathrm{He}(\alpha,\gamma)^7\mathrm{Be}$ radiative capture

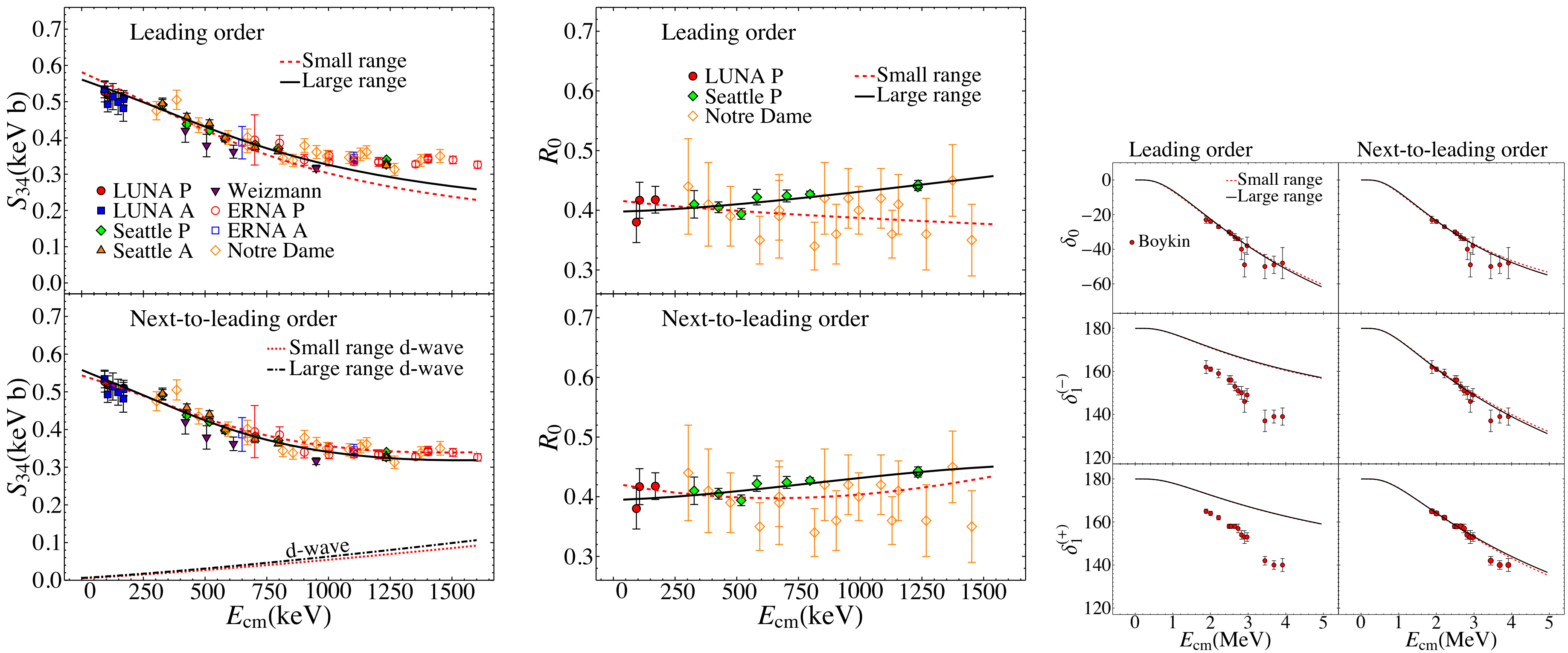

"Small range": capture to 500 keV, S-wave scatt to 2.5 MeV

"Large range": capture to 1000 keV, S-wave scatt to 3.0 MeV

$S_{34} \sim 0.55$ keV b

(RH, G. Rupak, A. Vaghani, EPJA 54, 89)

$^3\mathrm{He}(\alpha,\gamma)^7\mathrm{Be}$ radiative capture

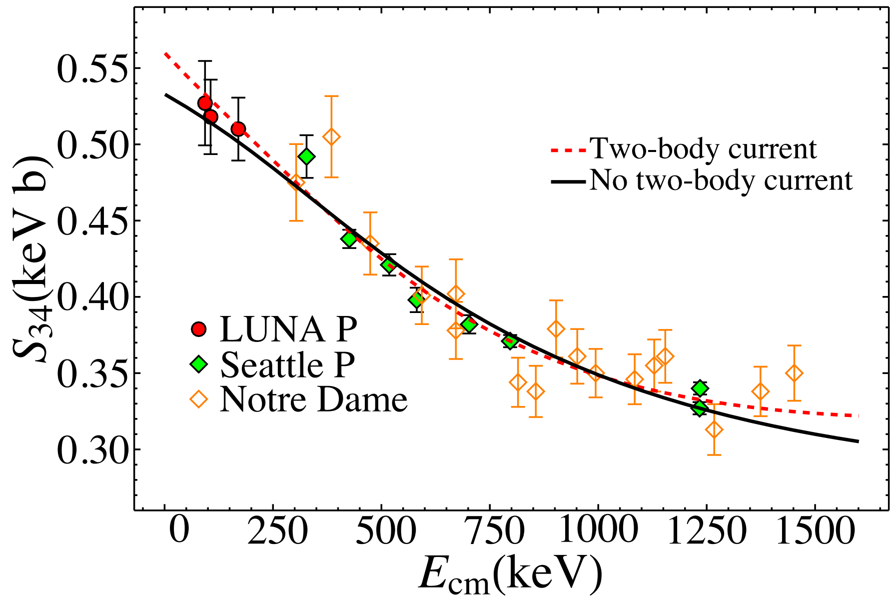

Strong correlation between two-body currents and renormalization constant (ANCs)

(RH, G. Rupak, A. Vaghani, EPJA 54, 89)

Efimov spectrum: how to probe?

- $E^{(n)}/E^{(n+1)} \sim 515$, too large!
- however, excited He trimers observed
  (Kunitski *et al.*, Science 348 (2015), 551)
- in nuclear physics: **virtual states**
  (Adhikari, Fonseca, Tomio, PRC26, 77;
  Yamashita, Frederico, Tomio, PLB 660, 339)
- our work: Rupak, Vaghani, RH, van Kolck, arXiv: 1806.01999 [nucl-th]

background: doublet nd scattering

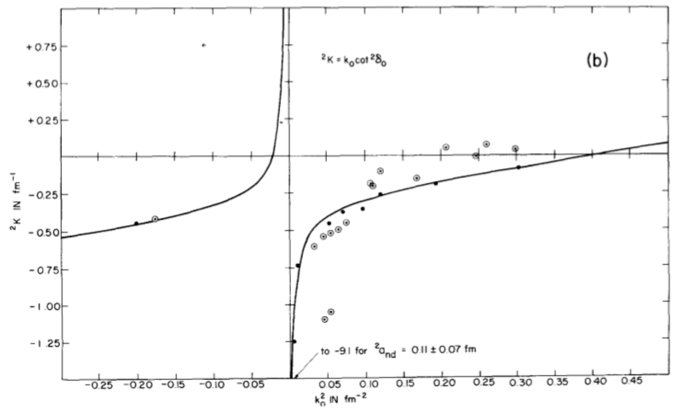

van Oers, Seagrave

- van Oers and Seagrave, PLB 24, 562 (1967)
- Whiting and Fuda, PRC 14, 18 (1976)
- Girard and Fuda, PRC 19, 579 (1969)
- Adhikari and Torreão, PLB 132, 257 (1983)
- Adhikari, Fonseca, Tomio, PRC 26, 77 (1982)

van Oers and Seagrave:

$$k \cot \delta - ik = \frac{2\pi}{\mu T} \approx -\frac{R}{1 + k^2/k_0^2} - A + Bk^2 - ik$$

halo/cluster EFT for nd

- idea: obtain the doublet nd scattering phase shifts from $\not{\pi}$EFT
- fits to determine the halo EFT couplings
- track the virtual state as γ_d decreases

halo/cluster EFT for nd

- T-matrix pole structure:

$$2ik\,\frac{\mu T}{2\pi} = \frac{2ik}{\frac{-1/a_{nd}+r_{nd}k^2/2}{1+k^2/k_0^2} - ik} = -2k\frac{k^2+k_0^2}{(k-i\,\kappa_1)(k-i\,\kappa_2)(k-i\,\kappa_3)}$$

- S-matrix residues:

$$\begin{aligned} iR_1 &= 2\kappa_1\frac{\kappa_1^2-k_0^2}{(\kappa_2-\kappa_1)(\kappa_3-\kappa_1)} < 0\,, \\ iR_2 &= -2\kappa_2\frac{\kappa_2^2-k_0^2}{(\kappa_2-\kappa_1)(\kappa_3-\kappa_2)} < 0\,, \\ iR_3 &= 2\kappa_3\frac{\kappa_2^2-k_0^2}{(\kappa_3-\kappa_1)(\kappa_3-\kappa_2)} > 0\,. \end{aligned}$$

κ_2: redundant pole [Ma, PR 71, 195 (1947)]

halo/cluster EFT for nd

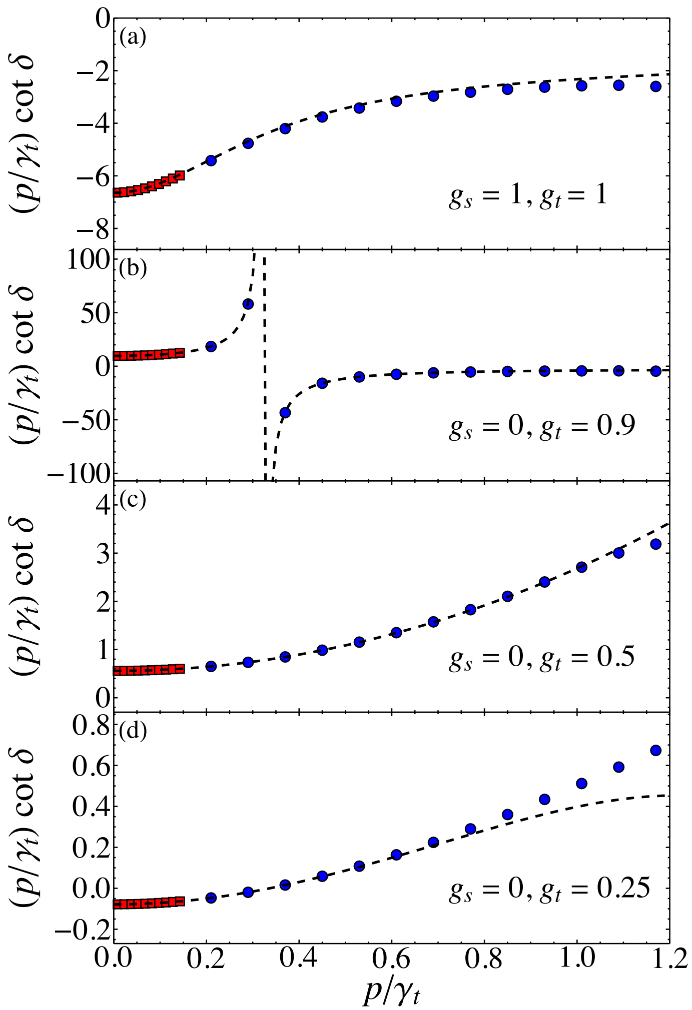

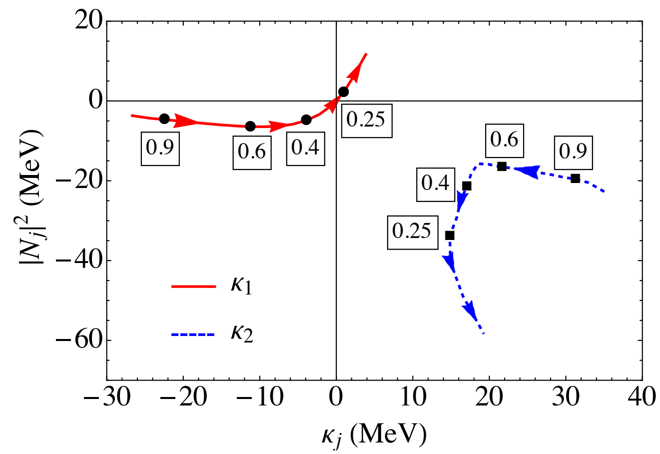

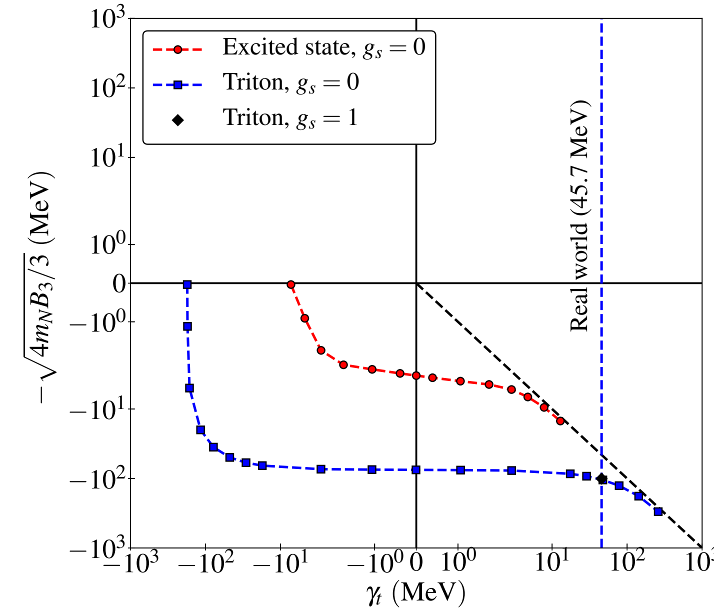

Casimir-Polder interaction between two neutral objects

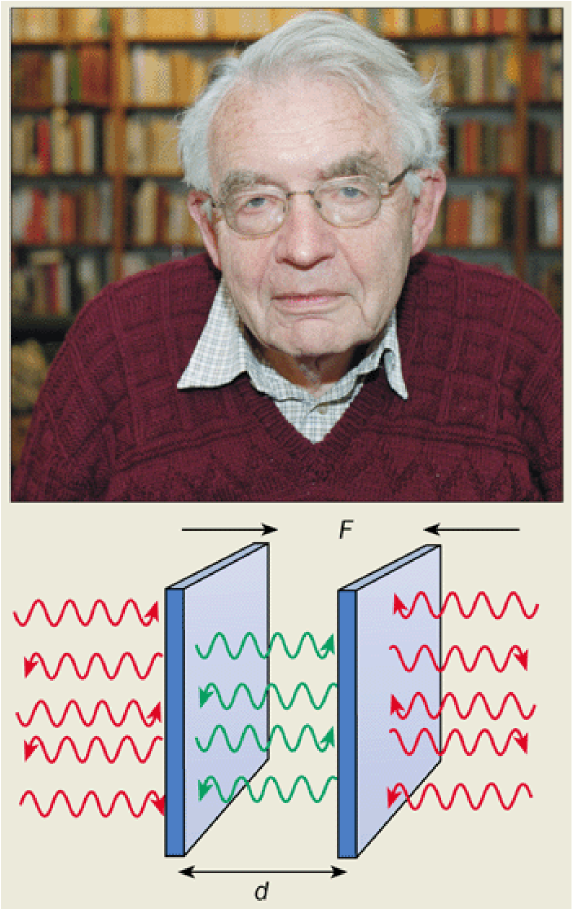

Casimir

Welton & Weisskopf

Schwinger

...

Casimir-Polder interaction between two neutral objects

Feinberg & Sucher, PRA 2, 2395 (1970), Spruch & Kelsey, PRA 18, 845 (1978)

$$V_{CP;ij}(r) = -\frac{\alpha_0}{\pi r^6} I_{ij}(r)\,,$$

$$I_{ij}(r) = \int_0^\infty d\omega\, e^{-2\alpha_0 \omega r} \Big\{ \Big[\alpha_i(i\omega)\alpha_j(i\omega) + \beta_i(i\omega)\beta_j(i\omega) \Big] P_E(\alpha_0 \omega r) + \Big[\alpha_i(i\omega)\beta_j(i\omega) + \beta_i(i\omega)\alpha_j(i\omega) \Big] P_M(\alpha_0 \omega r) \Big\}\,,$$

$$P_E(x) = x^4 + 2x^3 + 5x^2 + 6x + 3\,, \quad P_M(x) = -(x^4 + 2x^3 + x^2)\,.$$

neutron-neutron: (Tarrach, Ericson, NPA294, 417 (1978))

$$V_{CP,nn}(r \to \infty) \sim -\frac{1}{4\pi r^7} \Big[23(\alpha_n^2 + \beta_n^2) - 14\alpha_n \beta_n \Big]$$

Our fits:

(J. F. Babb, RH, M. S. Hussein, EPJA 53, 126 (2017))

	$\alpha_n(0)$ (10^{-4}fm^3)	$\beta_n(0)$ (10^{-4}fm^3)
Set 1 (fit parameter)	13.9968	4.2612
Set 2 (PDG)	11.6	3.7
Set 3 (Kossert *et al.*, 2003)	12.5	2.7

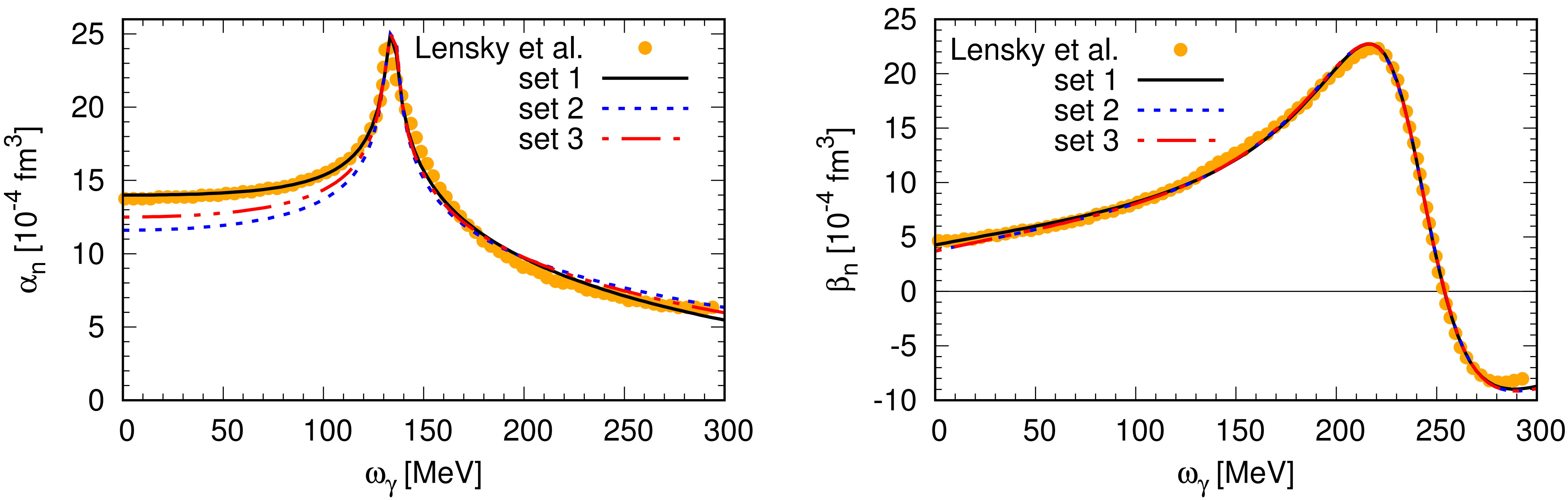

neutron-neutron Casimir-Polder interaction

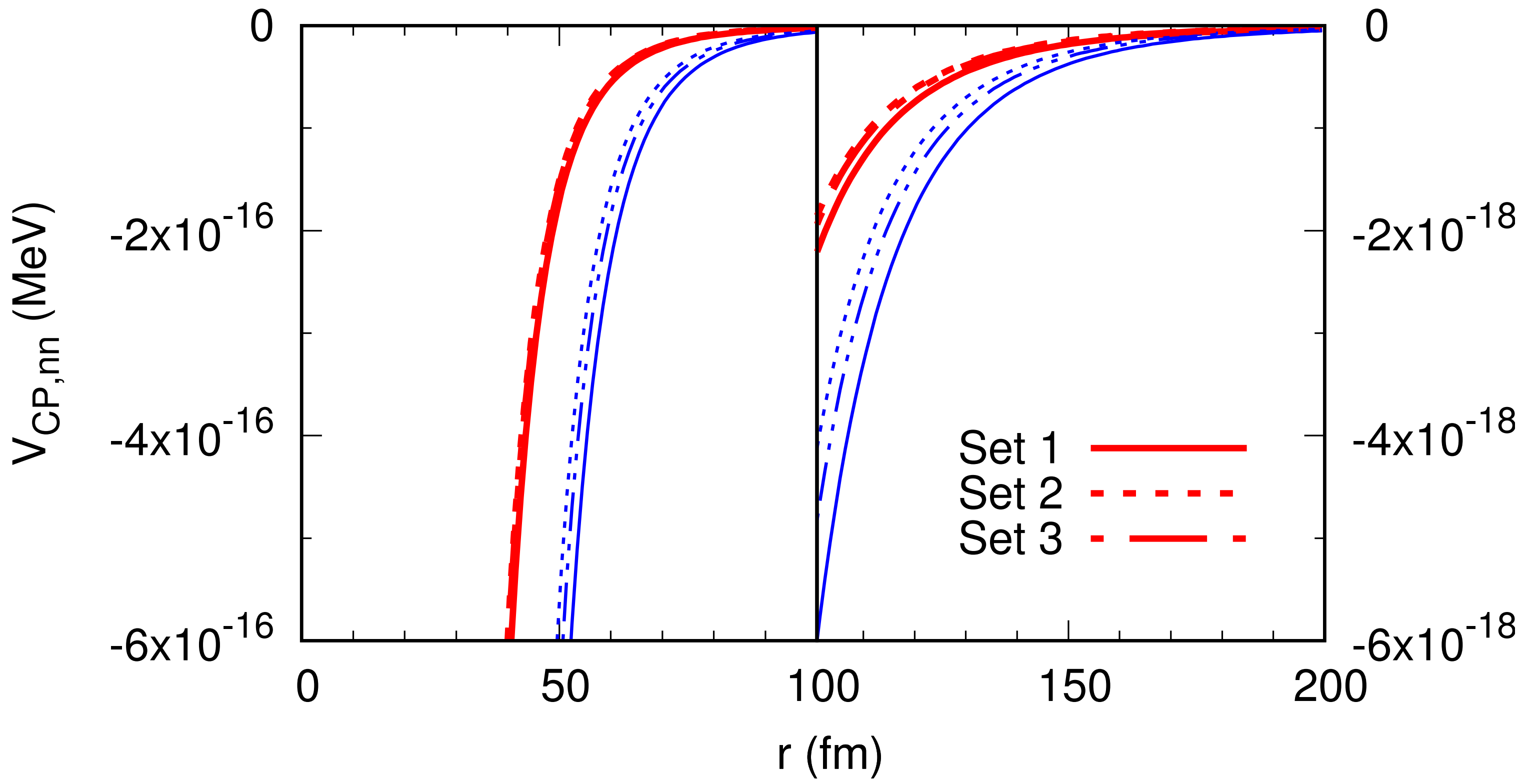

Thin blue curve: static limit of the polarizabilities ($V^{\star}_{CP,nn}$)

neutron-neutron Casimir-Polder interaction

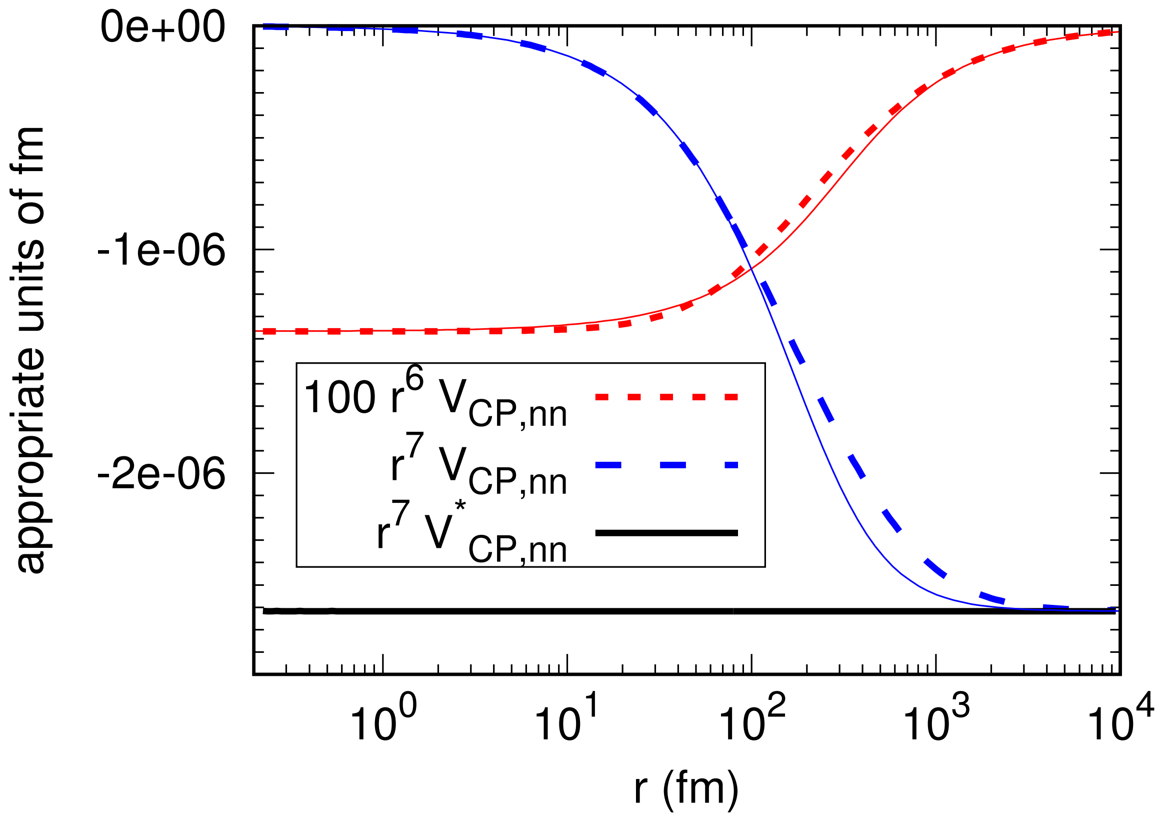

Thin continuous lines: arctan parametrization (O'Carroll & Sucher 69, Arnold 73)

neutron-Wall Casimir-Polder interaction

(Zhou & Spruch, PRA 52, 297 (95).)

$$V_{CP,nW}(r) = -\frac{\alpha_0}{4\pi r^3} J_{nW}(r), \quad J_{nW}(r) = \int_0^\infty d\omega\, e^{-2\alpha_0 \omega r} \alpha_n(i\omega) Q(\alpha_0 \omega r), \quad Q(x) = 2x^2 + 2x + 1$$

Thin blue curve: static limit of the polarizabilities ($V^\star_{CP,nW}$)

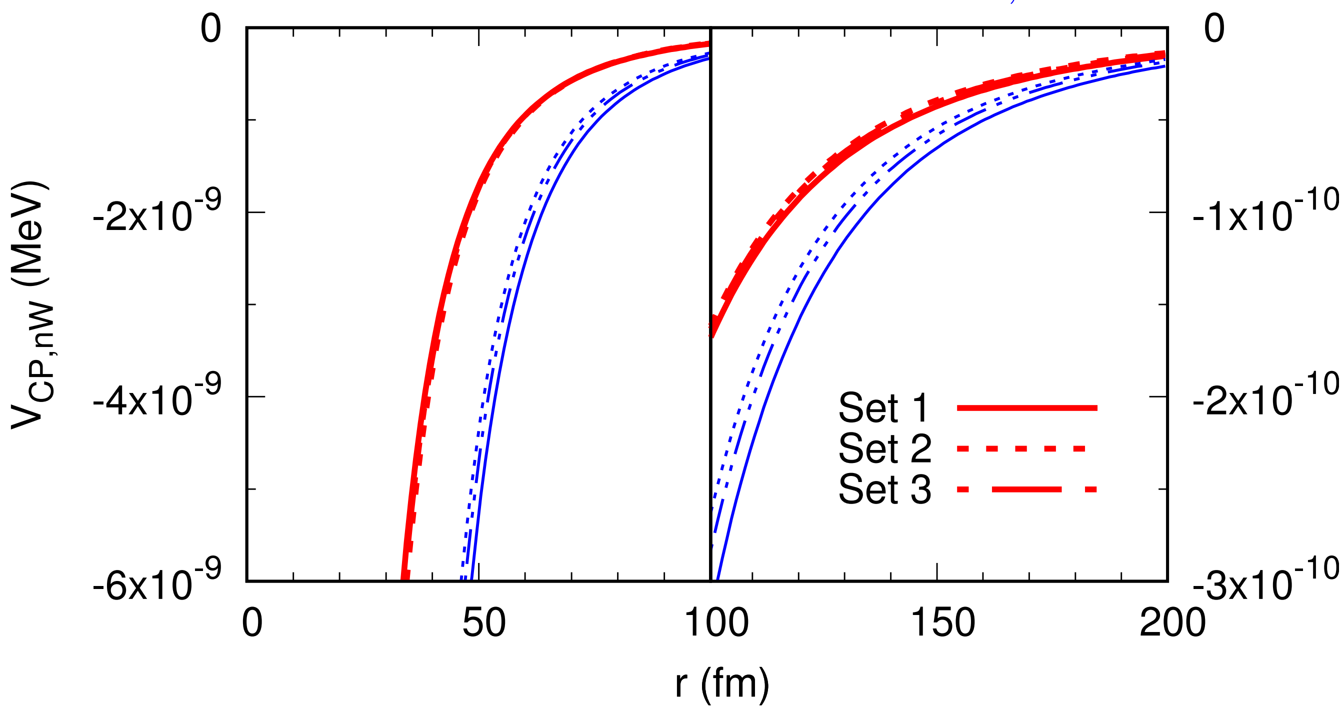

Wall-neutron-Wall

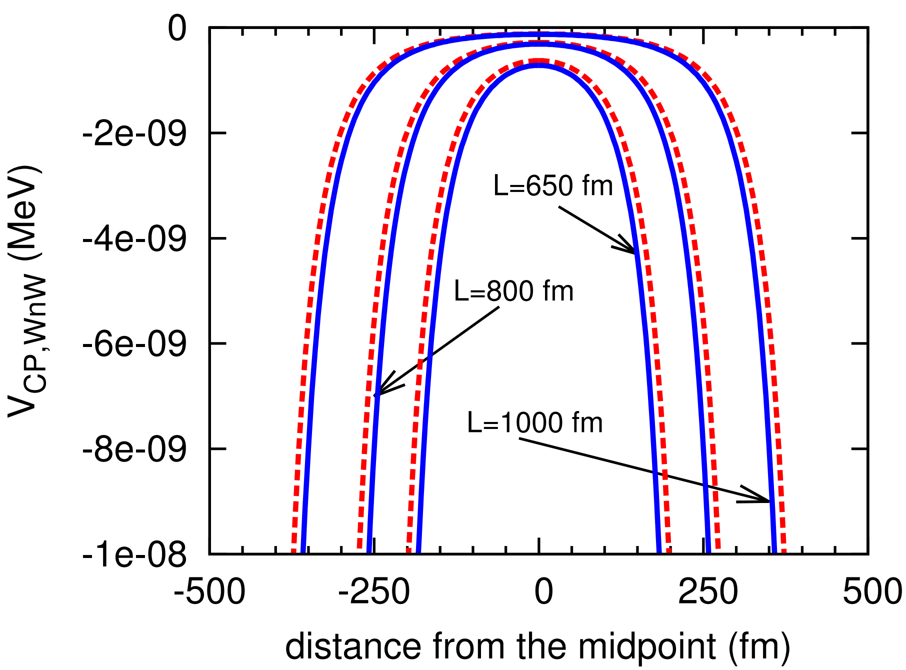

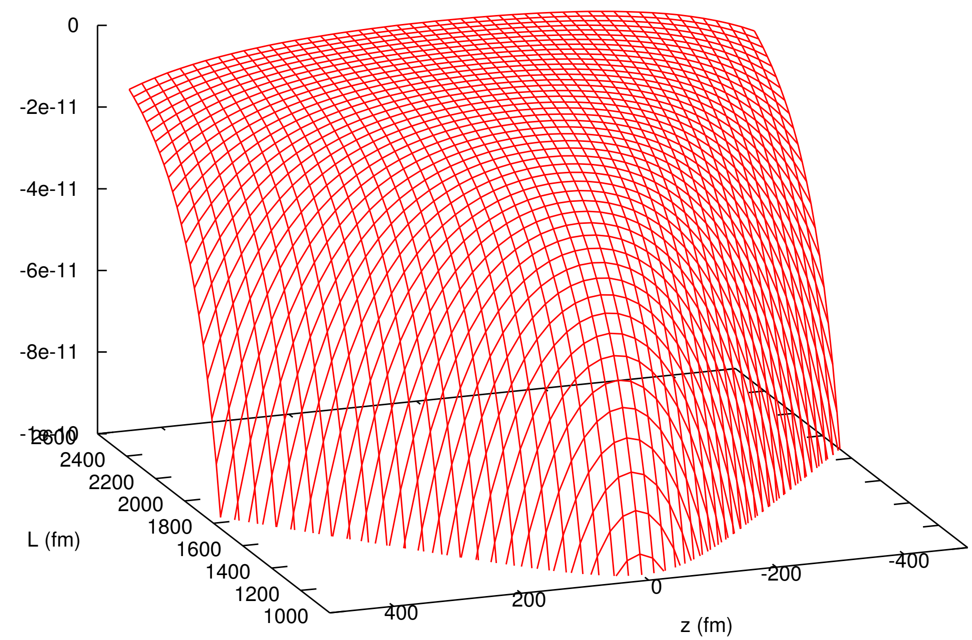

Summary

- halo/cluster EFT: systematic way, few-body correlations, EM/W currents
- $\alpha\alpha$ scattering:
  - Coulomb turned off $\Rightarrow$ conformal invariance @LO, Efimov spectrum in ^{12}C
  - incredible amount of fine-tuning
  - extraction of the ERE parameters with improved errorbars
- $^7\mathrm{Li}(n,\gamma)^8\mathrm{Li}$:
  - gauge invariance: cancellation of power divergences
  - "normalization" is very sensitive to r_1 (not well-known from elastic scatt.)
  - potential models: not so reliable extrapolations at low energies, uncontrolled theoretical uncertainties
  - excellent agreement with most recent MSU data (CD)

- $^3\mathrm{Li}(\alpha,\gamma)^7\mathrm{Be}$:
  - lack of scattering data low energies ($<$ 2 MeV)
  - lack of improved PWA (TRIUMF proposal)
  - reasonable agreement, but capture data sparse
- nd scattering:
  - two-dimer theory $\Rightarrow$ reproduces van Oers-Seagrave parametrization
  - keeps track of the zero in T and the virtual state
  - Efimov nature of the virtual state in a model-independent way
- Casimir-Polder interaction:
  - dipole polarizabilities - fit to RB-χEFT of Lensky *et al.* up to the onset of Δ $\Rightarrow$ improvement over the arctan param.
  - n-Wall and Wall-n-Wall - UCN, confinement in bottles, nanowires, etc.
- Perspectives: n-d, p-^{7}Be, 3α, Borromean halos, heavier nuclei, ...

the n-^{7}Li system

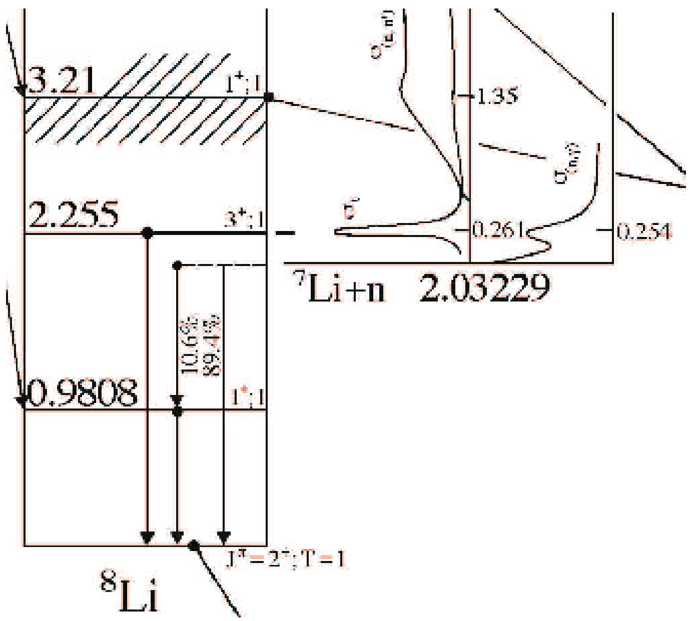

$\Rightarrow$ Bound states:

- 2^+ $(-2.03$ MeV$)$: $\frac{1}{\sqrt{2}}[^5P_2 + {}^3P_2]$ $(p_{3/2})$
- 1^+ $(-1.05$ MeV$)$: $\frac{1}{\sqrt{2}}[^5P_2 - {}^3P_2]$ $(p_{1/2})$

$\Rightarrow$ Scattering states:

- $^5S_2$: $a_0^{(2)} = -3.63 \pm 0.05$ fm
- $^3S_1$: $a_0^{(1)} = 0.87 \pm 0.07$ fm
- $^3P_3$: $E_R = 0.222$ MeV, $\Gamma_R = 0.031$ MeV

$\Rightarrow$ Radiative capture:

- $^5S_2, {}^5S_2 \rightarrow 2+$ (E1, 89.4%)
- $^5S_2, {}^5S_2 \rightarrow 1+$ (E1, 10.6%)
- $^5P_3 \rightarrow 2+$ (M1)

the n-$^7\mathrm{Li}$ system

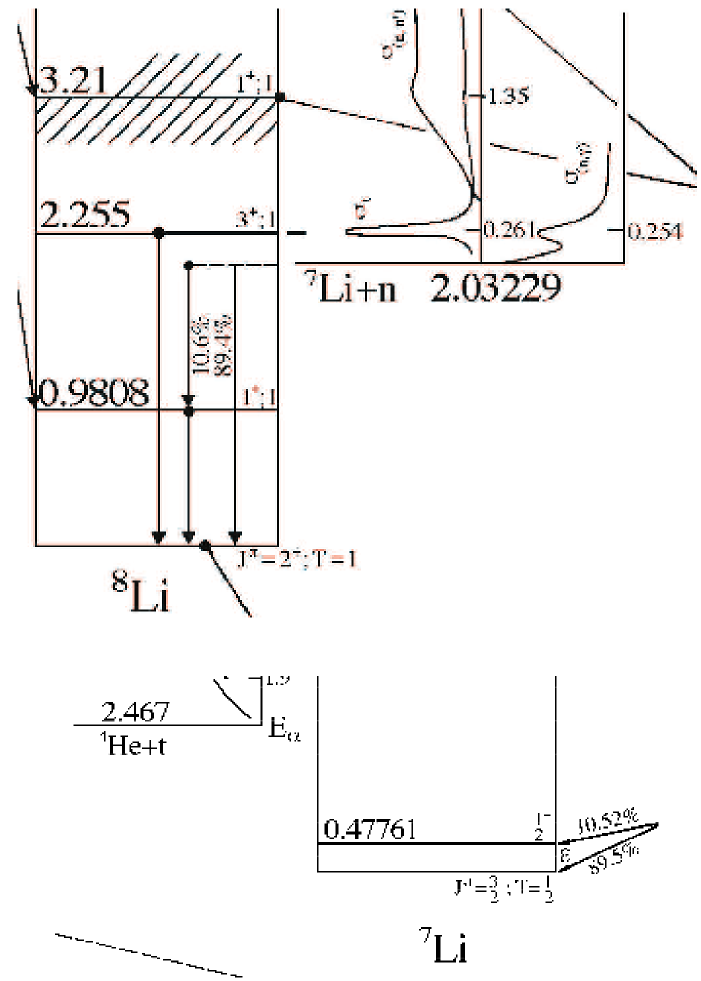

⇒ Bounded states:

- 2^+ (-2.03 MeV): $\frac{1}{\sqrt{2}}[{}^5P_2 + {}^3P_2]$ $(p_{3/2})$
- 1^+ (-1.05 MeV): $\frac{1}{\sqrt{2}}[{}^5P_2 - {}^3P_2]$ $(p_{1/2})$

⇒ Scattering states:

- ${}^5S_2$: $a_0^{(2)} = -3.63 \pm 0.05$ fm
- ${}^3S_1$: $a_0^{(1)} = 0.87 \pm 0.07$ fm
- ${}^3P_3$: $E_R = 0.222$ MeV, $\Gamma_R = 0.031$ MeV

⇒ Radiative capture:

- ${}^5S_2, {}^5S_2 \to 2+$ (E1, 89.4%)
- ${}^5S_2, {}^5S_2 \to 1+$ (E1, 10.6%)
- ${}^5P_3 \to 2+$ (M1)

halo/cluster EFT for n-$^7\mathrm{Li}$ (scatt. states)

$$\mathcal{L}_{\mathrm{kin}} = N^\dagger\left[i\partial_0+\frac{\vec{\nabla}^2}{2M_N}\right]N+C^\dagger\left[i\partial_0+\frac{\vec{\nabla}^2}{2M_C}\right]C\,,$$

$$\mathcal{L}_{\mathrm{int},s} = \phi_i^{(s)\dagger}\left[\underbrace{i\partial_0+\frac{\vec{\nabla}^2}{8\mu}}_{\sim C_2}-\underbrace{\Delta}_{\sim C_0}\right]\phi_i^{(s)}+g_0\left[\phi_i^{(s)\dagger}N^T\tilde{P}_i^{(s)}C+\mathrm{H.c.}\right]+\cdots\,,$$

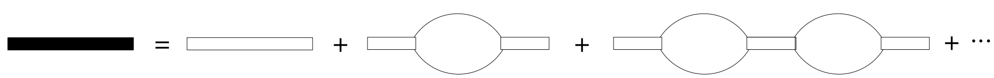

$$\Delta \sim \frac{M_{hi}^2}{\mu} \quad\rightarrow\quad iD_s^{(0)} = \frac{i}{-\Delta+i\epsilon} \sim \frac{\mu}{M_{hi}^2} \qquad (^3S_1)$$

$$\Delta \sim \frac{M_{hi}^2}{\mu}\frac{M_{lo}}{M_{hi}} \quad\rightarrow\quad iD_s^{(0)} = \frac{i}{-\Delta+i\epsilon} \sim \frac{\mu}{M_{hi}M_{lo}} \qquad (^5S_2)$$

halo/cluster EFT for n-$^7\mathrm{Li}$ (bound state)

p-wave: Bertulani, Hammer, van Kolck; Bedaque, Hammer, van Kolck

- two operators at LO!

$$\mathcal{L}_{\mathrm{int},p} = \phi_{ij}^{(p)\dagger}\left[i\partial_0 + \frac{\vec{\nabla}^2}{8\mu} - \Delta\right]\phi_{ij}^{(p)} + g_1\left[\phi_{ij}^{(p)\dagger} N^T \tilde{P}_{ij}^{(p)} C + \mathrm{H.c.}\right] + \cdots ,$$

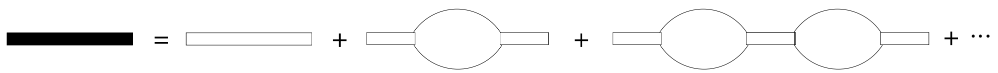

$$\Delta \sim M_{lo}^2/\mu \quad \to \quad iD_p^{(0)} = \frac{i}{q_0 - \boldsymbol{q}^2/8\mu - \Delta + i\epsilon} \sim \frac{\mu}{M_{lo}^2} \qquad ({}^3P_2, {}^5P_2)$$

$$\mathbf{D}_p = \frac{i}{q_0 - \boldsymbol{q}^2/8\mu - \Delta - 6g_1^2 L} \quad \Rightarrow \quad \mathcal{Z}^{-1} \equiv \frac{\partial}{\partial q_0}\left[\mathbf{D}_p^{-1}\right]_{\mathrm{pole}} = \frac{-2\pi}{3(\gamma_B + r_1)}$$

pole: $\boldsymbol{q} = 0$; $q_0 = -\gamma_B^2/2\mu$

halo/cluster EFT for nd

$$\mathcal{L} = N^\dagger \left[i\partial_0 + \frac{\vec{\nabla}^2}{2M_N} \right] N$$

$$+ \sum_{i=1}^{2} \phi_i^\dagger \left[\Delta_i + c_i \left(i\partial_0 + \frac{\vec{\nabla}^2}{6M} \right) \right] \phi_i + \sqrt{\frac{4\pi}{M}} \left[\phi_i^\dagger N^T P N + \text{H.c.} \right] + \cdots ,$$

$$c_1 \ll c_2 \qquad \Rightarrow \qquad k_0^2 = \frac{2\mu}{c_2} \left(\Delta_1 + \Delta_2 \right) \left(1 + \cdots \right) \sim \Omega^2$$

$$\kappa_1 = -\sqrt{\frac{2\mu\Delta_2}{c_2}} \left[1 - \frac{1}{2\Delta_2} \sqrt{\frac{2\mu\Delta_2}{c_2}} + \cdots \right] \sim \aleph$$

HB-χEFT: Hildebrandt *et al.*, EPJA 20, 290 (2004)

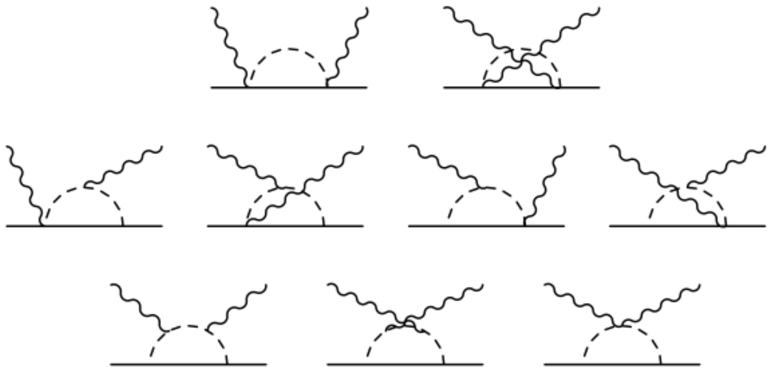

Fig. 2. Leading-one-loop $N\pi$ continuum contributions to nucleon polarizabilities.

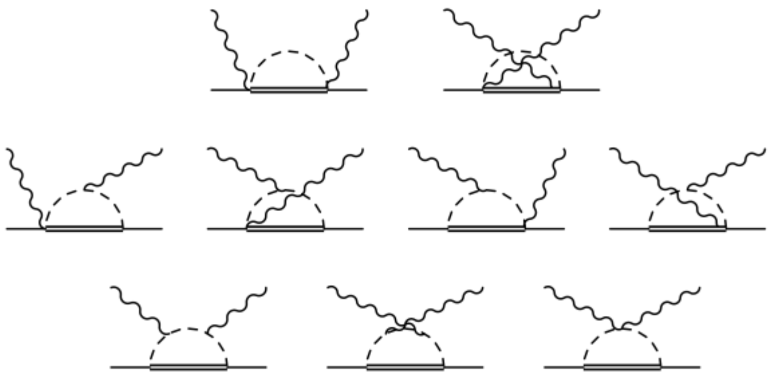

Fig. 3. Leading-one-loop $\Delta\pi$ continuum contributions to nucleon polarizabilities.

Fig. 4. Δ-pole and short-distance contributions to nucleon polarizabilities.

one-pion production threshold

$$\omega_\pi = \frac{m_\pi^2 + 2m_\pi M}{2(m_\pi + M)} \approx 131 \text{ MeV} \qquad (3.7)$$

is therefore not at the correct location. We correct for

HB-χEFT: Hildebrandt *et al.*, EPJA 20, 290 (2004)

The authors acknowledge helpful discussions with N. Kaiser, M.J. Savage, M. Schumacher and W. Weise. We are grateful to the ECT* in Trento for its hospitality where a large part of the work was done. This work was supported in part by the Bundesministerium für Forschung und Technologie, and by the Deutsche Forschungsgemeinschaft under contract GR1887/2-1 (H.W.G. and R.P.H.).

Appendix A. Projection formulae in Dispersion Theory

In this appendix, we give the relevant formulae to calculate the multipole amplitudes for Compton scattering from the invariant amplitudes A_i^{L}. Following the notation of ref. [5], we introduce the following six independent helicity amplitudes $\phi_{\Lambda'\Lambda}$, with $\Lambda = \lambda_\gamma - \lambda_N$ ($\Lambda' = \lambda'_\gamma - \lambda'_N$) related to the helicities of the initial (final) photon and nucleon, λ_γ (λ'_γ) and λ_N (λ'_N), respectively,

$$\begin{aligned}
\phi_1 &\equiv \phi_{1/2\,1/2}\,,\\
\phi_2 &\equiv \phi_{1/2\,-1/2}\,,\\
\phi_3 &\equiv \phi_{1/2\,-3/2}\,,\\
\phi_4 &\equiv \phi_{1/2\,3/2}\,,\\
\phi_5 &\equiv \phi_{3/2\,3/2}\,,\\
\phi_6 &\equiv \phi_{3/2\,-3/2}\,.
\end{aligned} \tag{A.1}$$

The invariant amplitudes A_i^{L} are connected to the helicity amplitudes ϕ_i by the relations

$$\begin{aligned}
\phi_1 &= \frac{\sqrt{(1-\sigma)}}{8\pi\sqrt{s}}\,\frac{(s-M^2)[2(s-M^2)+t]}{2M^3[M^2\sigma - s(\sigma-2)]}\\
&\quad\times\{(\sigma-1)s[2M^2 A_3^{\mathrm{L}} - (s-M^2)A_4^{\mathrm{L}}]\\
&\quad+2M^2 A_6^{\mathrm{L}}(\sigma M^2 - s)\},\\
\phi_2 &= -\frac{\sqrt{\sigma}}{8\pi\sqrt{s}}\,\frac{(s-M^2)^2}{4M^2 s^{3/2}}\\
&\quad\times\{-2M^2\sigma[A_1^{\mathrm{L}}(s+M^2)+A_2^{\mathrm{L}}(s-M^2)]\\
&\quad+sA_5^{\mathrm{L}}(\sigma-2)[2(s-M^2)+t]\},\\
\phi_3 &= -\frac{\sigma\sqrt{1-\sigma}}{8\pi\sqrt{s}}\,\frac{(s-M^2)^2}{4Ms}\\
&\quad\times\{4M^2 A_1^{\mathrm{L}} - A_5^{\mathrm{L}}[2(s-M^2)+t]\},\\
\phi_4 &= \frac{\sqrt{\sigma}\,(1-\sigma)}{8\pi\sqrt{s}}\,\frac{\sqrt{s}(s-M^2)[2(s-M^2)+t]}{2M^2[M^2\sigma - s(\sigma-2)]}\\
&\quad\times[2M^2 A_6^{\mathrm{L}} + A_3^{\mathrm{L}}(s+M^2)],\\
\phi_5 &= -\frac{(1-\sigma)\sqrt{(1-\sigma)}}{8\pi\sqrt{s}}\,\frac{s(s-M^2)[2(s-M^2)+t]}{M[M^2\sigma - s(\sigma-2)]}\\
&\quad\times\left[A_3^{\mathrm{L}} + A_6^{\mathrm{L}} + A_4^{\mathrm{L}}\frac{(s-M^2)}{2M^2}\right],\\
\phi_6 &= \frac{\sigma\sqrt{\sigma}}{8\pi\sqrt{s}}\,\frac{(s-M^2)^2}{4s\sqrt{s}}\,\{2(s-M^2)A_2^{\mathrm{L}}\\
&\quad-2A_1^{\mathrm{L}}(s+M^2) + A_5^{\mathrm{L}}[2(s-M^2)+t]\},
\end{aligned} \tag{A.2}$$

where $\sigma = -s\,t/(s-M^2)^2 = \sin^2(\theta/2)$.

The helicity amplitudes have the following standard partial-wave decomposition in terms of the reduced matrices $d^J_{\Lambda\Lambda'}$:

$$\phi_{\Lambda'\Lambda} = \sum_J (2J+1)\phi^J_{\Lambda'\Lambda}\, d^J_{\Lambda'\Lambda}(\theta), \tag{A.3}$$

which, by inversion, gives

$$\phi^J_{\Lambda'\Lambda} = \frac{1}{2}\int_{-1}^{+1} \mathrm{d}\cos\theta\;\; \phi_{\Lambda'\Lambda}(\cos\theta) d^J_{\Lambda'\Lambda}(\theta). \tag{A.4}$$

With the partial-wave decomposition of eq. (A.3), we finally obtain the relations between the multipole amplitudes of Compton scattering and the helicity partial waves:

$$\begin{aligned}
f^{l+}_{EE} &= \frac{1}{(l+1)^2}\left[\frac{1}{2}\left(\phi_1^{l+1/2} - \phi_2^{l+1/2}\right)\right.\\
&\quad\left.+\sqrt{\frac{l+2}{l}}\left(\phi_3^{l+1/2} - \phi_4^{l+1/2}\right) + \frac{l+2}{2l}\left(\phi_5^{l+1/2} - \phi_6^{l+1/2}\right)\right],\\
f^{l+}_{MM} &= \frac{1}{(l+1)^2}\left[\frac{1}{2}\left(\phi_1^{l+1/2} + \phi_2^{l+1/2}\right)\right.\\
&\quad\left.-\sqrt{\frac{l+2}{l}}\left(\phi_3^{l+1/2} + \phi_4^{l+1/2}\right) + \frac{l+2}{2l}\left(\phi_5^{l+1/2} + \phi_6^{l+1/2}\right)\right],\\
f^{l-}_{EE} &= \frac{1}{l^2}\left[\frac{1}{2}\left(\phi_1^{l-1/2} + \phi_2^{l-1/2}\right) + \sqrt{\frac{l-1}{l+1}}\left(\phi_3^{l-1/2} + \phi_4^{l-1/2}\right)\right.\\
&\quad\left.+\frac{l-1}{2(l+1)}\left(\phi_5^{l-1/2} + \phi_6^{l-1/2}\right)\right],\\
f^{l-}_{MM} &= \frac{1}{l^2}\left[\frac{1}{2}\left(\phi_1^{l-1/2} - \phi_2^{l-1/2}\right) - \sqrt{\frac{l-1}{l+1}}\left(\phi_3^{l-1/2} - \phi_4^{l-1/2}\right)\right.\\
&\quad\left.+\frac{l-1}{2(l+1)}\left(\phi_5^{l-1/2} - \phi_6^{l-1/2}\right)\right],\\
f^{l+}_{EM} &= \frac{1}{(l+1)^2}\left[-\frac{1}{2}\left(\phi_1^{l+1/2} - \phi_2^{l+1/2}\right)\right.\\
&\quad\left.-\frac{1}{\sqrt{l(l+2)}}\left(\phi_3^{l+1/2} - \phi_4^{l+1/2}\right) + \frac{1}{2}\left(\phi_5^{l+1/2} - \phi_6^{l+1/2}\right)\right],\\
f^{l+}_{ME} &= \frac{1}{(l+1)^2}\left[-\frac{1}{2}\left(\phi_1^{l+1/2} + \phi_2^{l+1/2}\right)\right.\\
&\quad\left.+\frac{1}{\sqrt{l(l+2)}}\left(\phi_3^{l+1/2} + \phi_4^{l+1/2}\right) + \frac{1}{2}\left(\phi_5^{l+1/2} + \phi_6^{l+1/2}\right)\right].
\end{aligned} \tag{A.5}$$

Appendix B. Compton amplitudes to leading-one-loop order in χEFT

The formulae which connect the amplitudes R_i discussed in the text to the A_i^H basis usually used in χEFT calculations of nucleon Compton scattering read [7]

$$\begin{aligned}
A_1^H &= 4\pi\frac{W}{M}(R_1 + zR_2)\,,\\
A_2^H &= -4\pi\frac{W}{M}R_2\,,\\
A_3^H &= 4\pi\frac{W}{M}(R_3 + zR_4 + 2zR_5 + 2R_6)\,,\\
A_4^H &= 4\pi\frac{W}{M}R_4\,,\\
A_5^H &= -4\pi\frac{W}{M}(R_4 + R_5)\,,\\
A_6^H &= -4\pi\frac{W}{M}R_6\,.
\end{aligned} \tag{B.1}$$

As discussed in sect. 2.1 we need to know both the pole as well as the structure-dependent contributions to A_i^H.

The cm pole contributions to the Compton amplitudes A_1^H to A_6^H for the case of a proton target have been calculated up to leading-one-loop order in ref. [27]. For completeness, we list them here again ($\kappa = \frac{1}{2}(\kappa_v + \kappa_s)$):

$$\begin{aligned}
A_1^{\mathrm{pole}}(\omega,\, z) &= -\frac{e^2}{M} + \mathcal{O}(\epsilon^4)\,,\\
A_2^{\mathrm{pole}}(\omega,\, z) &= \frac{e^2\omega}{M^2} + \mathcal{O}(\epsilon^4)\,,\\
A_3^{\mathrm{pole}}(\omega,\, z) &= \frac{e^2\omega\,\left(1+2\kappa-(1+\kappa)^2 z\right)}{2M^2}\\
&\quad-\frac{e^2 g_A}{4\pi^2 f_\pi^2}\,\frac{\omega^3(1-z)}{m_\pi^2 + 2\omega^2(1-z)} + \mathcal{O}(\epsilon^4)\,,\\
A_4^{\mathrm{pole}}(\omega,\, z) &= -\frac{e^2\omega\,(1+\kappa)^2}{2M^2} + \mathcal{O}(\epsilon^4)\,,\\
A_5^{\mathrm{pole}}(\omega,\, z) &= \frac{e^2\omega\,(1+\kappa)^2}{2M^2}\\
&\quad-\frac{e^2 g_A}{8\pi^2 f_\pi^2}\,\frac{\omega^3}{m_\pi^2 + 2\omega^2(1-z)} + \mathcal{O}(\epsilon^4)\,,\\
A_6^{\mathrm{pole}}(\omega,\, z) &= -\frac{e^2\omega\,(1+\kappa)}{2M^2}\\
&\quad+\frac{e^2 g_A}{8\pi^2 f_\pi^2}\,\frac{\omega^3}{m_\pi^2 + 2\omega^2(1-z)} + \mathcal{O}(\epsilon^4).
\end{aligned} \tag{B.2}$$

Finally, we present explicit expressions for the leading-one-loop order structure-dependent SSE Compton amplitudes including the kinematical as well as the short-distance corrections discussed in sect. 3.2. The threshold correction was done as follows for each diagram in fig. 2: If the pion propagator in a loop integral exhibits a cut at $\omega = m_\pi$, one replaces ω in that propagator by eq. (3.8) in order to obtain the physically correct s-channel cut position at $\omega = \omega_\pi$. The u-channel contribution is unchanged. We are aware, that this procedure violates crossing symmetry, but the crossing violating effects in the u-channel are quite small. Formally, the terms correcting for the exact location of the pion threshold start to appear at $\mathcal{O}(p^4)$.

$$\begin{aligned}
\bar{A}_1^H(\omega,z) &= \frac{b_1^2 e^2\omega^2 z}{9M^2}\left(-\frac{1}{\omega_s - \Delta_0} + \frac{1}{\omega_u + \Delta_0}\right) + \frac{\alpha\,(g_{118}\,t - g_{117}\,\omega^2)}{2\pi f_\pi^2 M}\\
&+\frac{\alpha}{18\pi f_\pi^2}\int_0^1 \mathrm{d}x\int_0^1 \mathrm{d}y\Bigg\{9g_A^2\Bigg[m_\pi\,\pi + \frac{\pi\,(2m_\pi^2 - t)}{2\sqrt{-t}}\,\arctan\left(\frac{\sqrt{-t}}{2m_\pi}\right) + \frac{\omega_s - \omega}{8\,\omega_s\,\omega}\,(m_\pi^2\pi^2 - 4\,\omega_s\,\omega)\\
&+\frac{m_\pi^2}{2\omega_s\,\omega}\left(\omega\arccos^2\left(-\frac{\omega_s}{m_\pi}\right) - \omega_s\arccos^2\left(\frac{\omega}{m_\pi}\right)\right) - (1-y)\left(\frac{1}{c_u}\left[5c_u^2 - (1-y)\left(\omega^2x^2(1-y)\right.\right.\right.\\
&\left.\left.\left.+t\left(\frac{x}{2} + (1-x)\,y\right)\right)\right]\arccos\left(\frac{\omega x\,(1-y)}{d}\right) + \frac{1}{c_s}\left[5c_s^2 - (1-y)\left(\omega^2x^2(1-y) + t\left(\frac{x}{2} + (1-x)\,y\right)\right)\right]\\
&\times\arccos\left(\frac{\omega_s x\,(-1+y)}{d}\right)\right)\Bigg] + 16\,g_{\pi N\Delta}^2\Bigg[-2\,\Delta_0\ln m_\pi - 3\Delta_0\ln\sqrt{m_\pi^2 - t\,(1-x)\,x}\\
&+\sqrt{-m_\pi^2 + (\Delta_0 - \omega)^2}\,\ln R(\Delta_0 - \omega) + \sqrt{-m_\pi^2 + (\Delta_0 + \omega)^2}\,\ln R(\Delta_0 + \omega) - 2\sqrt{-m_\pi^2 + (\Delta_0 - \omega x)^2}\,\ln R(\Delta_0 - \omega x)\\
&-2\sqrt{-m_\pi^2 + (\Delta_0 + \omega x)^2}\,\ln R(\Delta_0 + \omega x) - \frac{(3\Delta_0^2 - 3m_\pi^2 + 4t\,(1-x)\,x)}{\sqrt{\Delta_0^2 - m_\pi^2 + t\,(1-x)\,x}}\,\ln\left(\frac{\Delta_0 + \sqrt{\Delta_0^2 - m_\pi^2 + t\,(1-x)\,x}}{\sqrt{m_\pi^2 - t\,(1-x)\,x}}\right)\\
&+\Bigg(\frac{1}{C_s}\left(5C_s^2 + \omega^2x^2(1-y)^2 + \frac{1}{2}tx\,(1-y) + t\,(1-x)\,(1-y)\,y\right)\ln\tilde{R}(\Delta_0 - \omega x\,(1-y)) + 10\Delta_0\ln d\\
&+\frac{1}{C_u}\left(5C_u^2 + \omega^2x^2(1-y)^2 + \frac{1}{2}tx\,(1-y) + t\,(1-x)\,(1-y)\,y\right)\ln\tilde{R}(\Delta_0 + \omega x(1-y))\Bigg)(1-y)\Bigg]\Bigg\} + \mathcal{O}(\epsilon^4)\,,
\end{aligned} \tag{B.3}$$

See equations (B.3) *above and* (B.4)-(B.8)

on the following pages

HB-χEFT: Hildebrandt *et al.*, EPJA 20, 290 (2004)

$$
\begin{aligned}
\bar{A}_2^H(\omega,z) ={}& \frac{b_1^2 e^2 \omega^2}{9M^2}\left(\frac{1}{\omega_s-\Delta_0}-\frac{1}{\omega_u+\Delta_0}\right) - \frac{\alpha\, g_{118}}{\pi f_\pi^2 M}\omega^2 + \frac{\alpha}{18\pi f_\pi^2}\int_0^1 \mathrm{d}x\int_0^1 \mathrm{d}y\,\omega^2(1-y)\Big\{9g_A^2\Big[(1-x)\,x \\
&\times\left(\frac{\omega_s}{c_s^2 d^2}-\frac{\omega}{c_u^2 d^2}\right)(1-y)^3 y\left(\omega^2x^2(1-y)+t\left(\frac{x}{2}+(1-x)\,y\right)\right) - \frac{1}{c_s^3}\Big((-1+x)\,(1-y)^2 y\Big(\omega^2x^2\,(1-y) \\
&+t\left(\frac{x}{2}+(1-x)\,y\right)\Big)+c_s^2\,(x\,y+(1-x)\,(1-7y+7y^2))\Big)\arccos\left(\frac{\omega_s x\,(-1+y)}{d}\right) - \frac{1}{c_u^3} \\
&\times\Big((-1+x)\,(1-y)^2 y\left(\omega^2x^2\,(1-y)+t\left(\frac{x}{2}+(1-x)\,y\right)\right)+c_u^2\,(x\,y+(1-x)\,(1-7y+7y^2))\Big)\arccos\left(\frac{\omega x\,(1-y)}{d}\right)\Big] \\
&-16\,g_{\pi N\Delta}^2\Big[(1-x)\left(\frac{-\Delta_0+\omega x\,(1-y)}{C_s^2d^2}-\frac{\Delta_0+\omega x\,(1-y)}{C_u^2d^2}\right)(1-y)^2y\left(\omega^2x^2\,(1-y)+\frac12 t\,x+t\,(1-x)\,y\right) \\
&+\frac{1}{C_s^3}\Big(C_s^2\,((1-x)\,(1-7y)\,(1-y)+y)+(1-x)\,(1-y)^2y\left(\omega^2x^2\,(1-y)+\frac12 t\,x+t\,(1-x)\,y\right)\Big) \\
&\times\ln\bar{R}\,(\Delta_0-\omega x\,(1-y))+\frac{1}{C_u^3}\Big(C_u^2\,((1-x)\,(1-7y)\,(1-y)+y)+(1-x)\,(1-y)^2y \\
&\times\left(\omega^2x^2\,(1-y)+\frac12 t\,x+t\,(1-x)\,y\right)\Big)\ln\bar{R}\,(\Delta_0+\omega x(1-y))\Big]\Big\}+\mathcal{O}\left(\epsilon^4\right),
\end{aligned}
\tag{B.4}
$$

$$
\begin{aligned}
\bar{A}_3^H(\omega,z) ={}& \frac{b_1^2 e^2 \omega^3 z}{18M^2\Delta_0}\left(\frac{1}{\omega_s-\Delta_0}-\frac{1}{\omega_u+\Delta_0}\right) + \frac{\alpha}{\pi f_\pi^2}\int_0^1 \mathrm{d}x\int_0^1 \mathrm{d}y\Big\{\frac{g_A^2}{2}\Big[-\frac{\omega_s+\omega}{8\,\omega_s\omega}\,(m_\pi{}^2\pi^2+4\,\omega_s\omega) \\
&+\frac{m_\pi{}^2}{2\,\omega_s\omega}\left(\omega\arccos^2\left(-\frac{\omega_s}{m_\pi}\right)+\omega_s\arccos^2\left(\frac{\omega}{m_\pi}\right)\right)+\omega^4\,(1-x)\,x\,(1-y)^3y\,(1-z^2) \\
&\times\left(\left(\frac{\omega_s}{c_s^2d^2}+\frac{\omega}{c_u^2d^2}\right)x\,(1-y)-\frac{1}{c_u^3}\arccos\left(\frac{\omega x\,(1-y)}{d}\right)+\frac{1}{c_s^3}\arccos\left(\frac{\omega_s x\,(-1+y)}{d}\right)\right)\Big] \\
&+\frac{4\,g_{\pi N\Delta}^2}{9}\Big[-\sqrt{-m_\pi^2+(\Delta_0-\omega)^2}\,\ln R(\Delta_0-\omega)+\sqrt{-m_\pi^2+(\Delta_0+\omega)^2}\,\ln R(\Delta_0+\omega) \\
&+2\sqrt{-m_\pi^2+(\Delta_0-\omega x)^2}\,\ln R(\Delta_0-\omega x)-2\sqrt{-m_\pi^2+(\Delta_0+\omega x)^2}\,\ln R(\Delta_0+\omega x)-\omega^4\,(1-x)\,x(1-y)^3\,y\,(1-z^2) \\
&\times\left(\frac{\Delta_0-\omega x\,(1-y)}{C_s^2d^2}-\frac{\Delta_0+\omega x\,(1-y)}{C_u^2d^2}-\frac{1}{C_s^3}\ln\bar{R}\,(\Delta_0-\omega x(1-y))+\frac{1}{C_u^3}\ln\bar{R}\,(\Delta_0+\omega x\,(1-y))\right)\Big]\Big\}+\mathcal{O}(\epsilon^4),
\end{aligned}
\tag{B.5}
$$

$$
\begin{aligned}
\bar{A}_4^H(\omega,z) ={}& \frac{b_1^2 e^2 \omega^3}{18M^2\Delta_0}\left(\frac{1}{\omega_s-\Delta_0}-\frac{1}{\omega_u+\Delta_0}\right) + \frac{\alpha}{\pi f_\pi^2}\int_0^1 \mathrm{d}x\int_0^1 \mathrm{d}y\,\omega^2x\,(1-y)^2\Big\{\frac{g_A^2}{2}\Big[-\frac{1}{c_u}\arccos\left(\frac{\omega x\,(1-y)}{d}\right) \\
&+\frac{1}{c_s}\arccos\left(\frac{\omega_s x\,(-1+y)}{d}\right)\Big]+\frac{4\,g_{\pi N\Delta}^2}{9}\left[-\frac{1}{C_s}\ln\bar{R}\,(\Delta_0-\omega x(1-y))+\frac{1}{C_u}\ln\bar{R}\,(\Delta_0+\omega x\,(1-y))\right]\Big\}+\mathcal{O}(\epsilon^4),
\end{aligned}
\tag{B.6}
$$

$$
\begin{aligned}
\bar{A}_5^H(\omega,z) ={}& \frac{b_1^2 e^2 \omega^3}{18M^2\Delta_0}\left(-\frac{1}{\omega_s-\Delta_0}+\frac{1}{\omega_u+\Delta_0}\right) + \frac{\alpha}{\pi f_\pi^2}\int_0^1 \mathrm{d}x\int_0^1 \mathrm{d}y\,\omega^2\,(1-y)y\Big\{\frac{g_A^2}{2}\Big[\omega^2\left(\frac{\omega_s}{c_s^2d^2}+\frac{\omega}{c_u^2d^2}\right) \\
&\times(1-x)\,x^2\,(1-y)^3z-\frac{1}{c_u^3}\left(-c_u^2+\omega^2\,(1-x)\,x\,(1-y)^2z\right)\arccos\left(\frac{\omega x\,(1-y)}{d}\right) \\
&+\frac{1}{c_s^3}\left(-c_s^2+\omega^2\,(1-x)\,x\,(1-y)^2z\right)\arccos\left(\frac{\omega_s x\,(-1+y)}{d}\right)\Big] \\
&+\frac{4\,g_{\pi N\Delta}^2}{9}\Big[\frac{1}{C_s}\ln\bar{R}\,(\Delta_0-\omega x(1-y))-\frac{1}{C_u}\ln\bar{R}\,(\Delta_0+\omega x\,(1-y))-\omega^2\,(1-x)\,x\,(1-y)^2z \\
&\times\left(\frac{\Delta_0-\omega x\,(1-y)}{C_s^2d^2}-\frac{\Delta_0+\omega x\,(1-y)}{C_u^2d^2}-\frac{1}{C_s^3}\ln\bar{R}\,(\Delta_0-\omega x(1-y))+\frac{1}{C_u^3}\ln\bar{R}\,(\Delta_0+\omega x\,(1-y))\right)\Big]\Big\}+\mathcal{O}(\epsilon^4),
\end{aligned}
\tag{B.7}
$$

$$
\begin{aligned}
\bar{A}_6^H(\omega,z) ={}& \frac{\alpha}{\pi f_\pi^2}\int_0^1 \mathrm{d}x\int_0^1 \mathrm{d}y\,\omega^2\,(1-y)\,y\Big\{\frac{g_A^2}{2}\Big[-\omega^2\left(\frac{\omega_s}{c_s^2d^2}+\frac{\omega}{c_u^2d^2}\right)(1-x)\,x^2\,(1-y)^3+\frac{1}{c_u^3}\Big(-c_u^2 \\
&+\omega^2\,(1-x)\,x(1-y)^2\Big)\arccos\left(\frac{\omega x\,(1-y)}{d}\right)-\frac{1}{c_s^3}\left(-c_s^2+\omega^2\,(1-x)\,x(1-y)^2\right)\arccos\left(\frac{\omega_s x\,(-1+y)}{d}\right)\Big] \\
&+\frac{4g_{\pi N\Delta}^2}{9}\Big[-\frac{1}{C_s}\ln\bar{R}\,(\Delta_0-\omega x\,(1-y))+\frac{1}{C_u}\ln\bar{R}\,(\Delta_0+\omega x(1-y))+\omega^2\,(1-x)\,x\,(1-y)^2 \\
&\times\left(\frac{\Delta_0-\omega x\,(1-y)}{C_s^2d^2}-\frac{\Delta_0+\omega x\,(1-y)}{C_u^2d^2}-\frac{1}{C_s^3}\ln\bar{R}\,(\Delta_0-\omega x\,(1-y))+\frac{1}{C_u^3}\ln\bar{R}\,(\Delta_0+\omega x(1-y))\right)\Big]\Big\}+\mathcal{O}(\epsilon^4).
\end{aligned}
\tag{B.8}
$$

In eqs. (B.3)-(B.8) we have used the following abbreviations:

$$
\begin{aligned}
d^2 &= m_\pi^2 - t\,(1-x)\,(1-y)\,y\,, \\
c_s^2 &= d^2-\omega_s^2x^2\,(1-y)^2\,, \\
c_u^2 &= d^2-\omega^2x^2\,(1-y)^2\,, \\
C_s^2 &= (\Delta_0-\omega x\,(1-y))^2-d^2\,, \\
C_u^2 &= (\Delta_0+\omega x\,(1-y))^2-d^2\,; \\
\omega_s &= \sqrt{s}-M\,, \\
\omega_u &= M-\sqrt{u}\,, \\
s &= (p+k)^2=\left(\omega+\sqrt{M^2+\omega^2}\right)^2\,, \\
t &= (k-k')^2=2\omega^2\,(z-1)\,, \\
u &= (p-k')^2=M^2-2\,\omega\sqrt{M^2+\omega^2}-2\,\omega^2z\,;
\end{aligned}
$$

$$
R(X)=\frac{X}{m_\pi}+\sqrt{\frac{X^2}{m_\pi^2}-1},\quad \bar{R}(X)=\frac{X}{d}+\sqrt{\frac{X^2}{d^2}-1}\,.
$$

For the *isovector* Compton structure amplitudes, one finds a null result to leading-one-loop order:

$$
\bar{A}_i^{H\,(v)}=0+\mathcal{O}(\epsilon^4)\,, \tag{B.5}
$$

with $i=1,\dots,6$.

Appendix C. Projection formulae for χEFT

The connection between the Compton structure amplitudes $\bar{A}_i^H(\omega,z)$, $i=1,\dots,6$ given in the previous section and the cm Compton multipoles $f_{XX'}^{l\pm}(\omega)$, $X,X'=E,M$, introduced in sect. 2.1, reads

$$
\begin{aligned}
f_{EE}^{1+}(\omega) ={}& \int_{-1}^{1}\frac{M}{16\cdot 4\pi\,W}\Big[\bar{A}_3^H(\omega,z)\,(-3+z^2) \\
&+4\bar{A}_6^H(\omega,z)\,(-1+z^2)+\Big(2\bar{A}_2^H(\omega,z)+\bar{A}_4^H(\omega,z) \\
&+2\,\bar{A}_5^H(\omega,z)\Big)\,z\,(-1+z^2)+2\bar{A}_1^H(\omega,z)\,(1+z^2)\Big]\mathrm{d}z\,,
\end{aligned}
$$

$$
\begin{aligned}
f_{EE}^{1-}(\omega) ={}& \int_{-1}^{1}\frac{M}{8\cdot 4\pi\,W}\Big[-\bar{A}_3^H(\omega,z)\,(-3+z^2) \\
&-4\bar{A}_6^H(\omega,z)\,(-1+z^2)-\Big(-\bar{A}_2^H(\omega,z)+\bar{A}_4^H(\omega,z) \\
&+2\,\bar{A}_5^H(\omega,z)\Big)\,z\,(-1+z^2)+\bar{A}_1^H(\omega,z)\,(1+z^2)\Big]\mathrm{d}z\,,
\end{aligned}
$$

$$
\begin{aligned}
f_{MM}^{1+}(\omega) ={}& \int_{-1}^{1}\frac{M}{16\cdot 4\pi\,W}\Big[2\bar{A}_2^H(\omega,z)\,(-1+z^2) \\
&+\bar{A}_4^H(\omega,z)\,(-1+z^2)+2\Big(\bar{A}_5^H(\omega,z)\,(1-z^2) \\
&+\bar{A}_1^H(\omega,z)\,2z-\bar{A}_3^H(\omega,z)\,z\Big)\Big]\mathrm{d}z\,,
\end{aligned}
$$

$$
\begin{aligned}
f_{MM}^{1-}(\omega) ={}& \int_{-1}^{1}\frac{M}{8\cdot 4\pi\,W}\Big[\bar{A}_4^H(\omega,z)\,(1-z^2) \\
&+\bar{A}_2^H(\omega,z)\,(-1+z^2)+2\Big(\bar{A}_5^H(\omega,z)\,(-1+z^2) \\
&+\bar{A}_1^H(\omega,z)\,z+\bar{A}_3^H(\omega,z)\,z\Big)\Big]\mathrm{d}z\,,
\end{aligned}
$$

$$
\begin{aligned}
f_{EE}^{2+}(\omega) ={}& \int_{-1}^{1}\frac{M}{72\cdot 4\pi\,W}\Big[\bar{A}_4^H(\omega,z)\,(-1-3z^2+4z^4) \\
&+\bar{A}_2^H(\omega,z)\,(3-9z^2+6z^4)+2\Big(\bar{A}_5^H(\omega,z) \\
&\times(-1-3z^2+4z^4)+\bar{A}_1^H(\omega,z)\,3z^3 \\
&+\bar{A}_3^H(\omega,z)\,(2z^3-3z)+\bar{A}_6^H(\omega,z)\,(6z^3-6z)\Big)\Big]\mathrm{d}z\,,
\end{aligned}
$$

neutron-Wall Casimir-Polder interaction

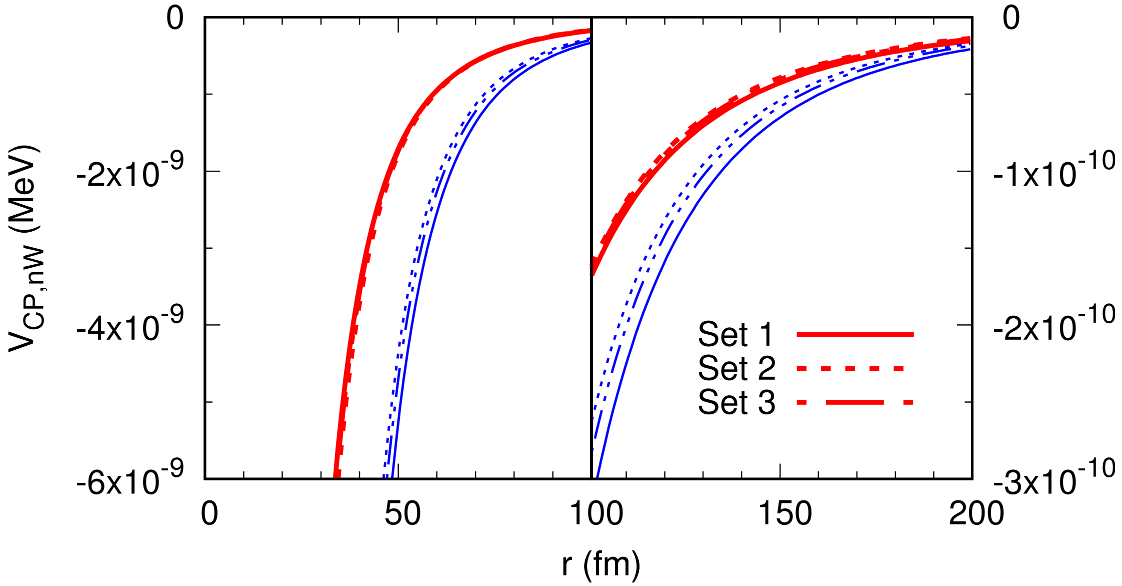

- UC neutrons: $v_n \sim$ 3-25 m/s
- Fermi pseudo-potential: $V_F = \rho a \left(2\pi\hbar^2/M_N\right)$ [Ni ≈ 252 neV, Al ≈ 54 neV]